IOSUD – Polytechnic University of Timisoara
Doctoral School of Engineering Studies

ENSURING THE ENERGY EFFICIENCY OF THERMAL SYSTEMS AND COMFORT IN CIVIL BUILDINGS USING THE GROUND-COUPLED HEAT PUMP

Doctoral Thesis – Abstract

for obtaining the scientific title of doctor at
Polytechnic University of Timisoara
in the field of PhD Civil Engineering and Building Services

author, eng. Alexandru DORCA
scientific leader Prof.univ.dr.eng. Ioan SARBU

September 2023

1. INTRODUCTION

Chapter 1 includes considerations on the subject and actuality of the thesis, the necessity and opportunity of the research, with reference to the importance of buildings from an energy point of view, in the context of sustainable development, which assumes as objectives: the reorientation of energy production technologies, the increase the resource base, the implementation of renewable energy resources (RES) and the reduction of carbon dioxide (CO_2) emissions. Statistical data show that of the total primary energy consumption of the European Union (EU), buildings represent 41%, followed by transport with 31% and industry with 28%, of which more than 50% is electricity. The main solutions and possibilities for reducing thermal energy in buildings are presented to ensure the conditions of adequate thermal comfort and the need to use heat pumps (HPs) is justified based on national and international legislation. The integration of RES (especially solar and geothermal energy) in space heating/cooling and domestic hot water production (DHW) is a good alternative for a clean environment to traditional solutions, and geothermal HP is one of the most advantageous systems to be considered for the use of heat taken from the ground and the reduction of CO_2 emissions, as well as for the transformation of existing buildings undergoing renovation into near-zero energy buildings (nZEB).

In the context of sustainable development, energy is one of the most prominent resources facing the contemporary world. The economic strategy of a sustainable development requires the promotion of energy efficiency and the rational use of energy at the level of buildings, a major consumer of energy at the level of both Romania and the EU member countries, but also the integration of RES [1–3], in the idea to save fossil fuels and reduce greenhouse gas (GHG) emissions. By 2030, the EU plans to reduce GHG emissions by 55% and increase its use of RES (solar, geothermal, wind, biomass, hydro and nuclear) to 40% [4].

The residential and tertiary building sectors (offices, commercial spaces, hotels, restaurants, schools, hospitals, gyms) are the largest final consumers of energy, especially for heating, cooling, ACC, lighting and appliances. Thus, buildings offer the greatest and most cost-effective energy saving potential. In this context, the reduction of energy consumption and GHG emissions represent two directions that have oriented study and investigation efforts in the field of building services engineering.

The key factors in minimizing energy consumption in buildings are: the energy source used for each consumer, the techniques applied within each use, the building design, the behavior and requirements of the users. The main solutions and measures to save energy are presented in Fig. 1.6.

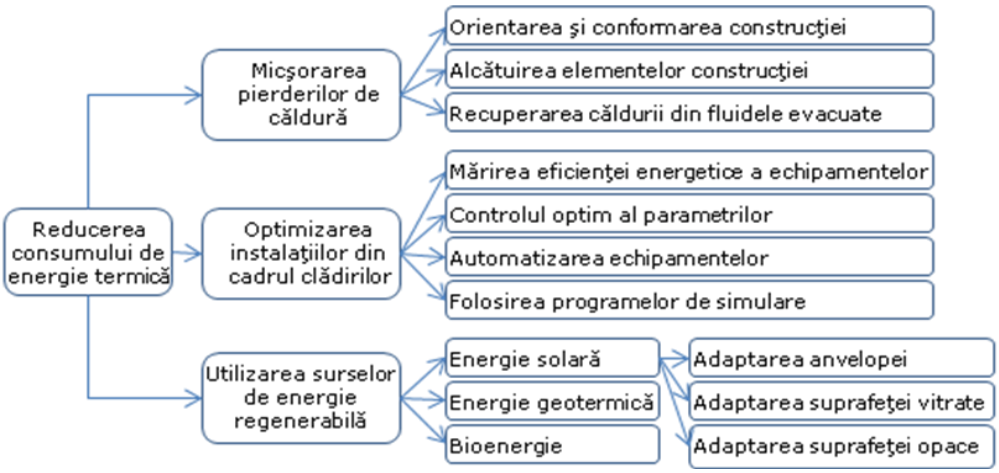

Fig. 1.6 Solutions and measures to reduce the thermal energy used in buildings

The functional-energy optimization of building services and the use of RES lead to important energy savings. In addition, increasing the share of energy consumed in buildings to 30% nationally and the share of renewable resources to 12.5% in EU member countries constitute fundamental arguments for exploration in the field of RES use to cover the hygiene and comfort needs of building occupants, the line on which the present doctoral thesis is also wrote.

Among RES, the most abundant and affordable energy is solar energy, captured directly from solar radiation with solar thermal collectors (ST), photovoltaic panels (PV) and photovoltaic–thermal panels (PV/T) or indirectly from soil, water and air.

When it comes to using high efficiency heating/cooling systems and SER integration, the heat pump (HP) is one of the most advantageous systems to consider in a heating, ventilation and air conditioning (HVAC) installation. The need to use HP in civil constructions is based on international and national legislation represented by the Kyoto Protocol (1997) [5] regarding the reduction of GHG emissions and Directive 2002/91/EC [6] regarding the energy performance of buildings transposed in Romania in Law 372/2005, amended and supplemented by Law 159/2013, which also includes HPs.

The most significant systems for extracting thermal energy from the ground are geothermal HPs [7,8], widely used in both residential and commercial buildings, their installation increasing globally from 10% to 30% annually in last decade [9].

In the context of sustainable development, the doctoral research started in 2016 has the main objective of ensuring the energy efficiency of thermal installations (heating, cooling, ACC) and comfort in civil buildings using HP with vapor compression coupled to the ground in a closed circuit through vertical collectors, in order to reduce energy consumption and CO_2 emissions. The PhD thesis aims to provide a more solid basis for the design of such systems in the future and thus to fill existing knowledge gaps for practical applications. A deep analysis of the performance of HPs connected to various heating/cooling systems for the conditions in Romania is extremely necessary also due to the fact that the results of international studies cannot be directly applied at the local level, due to the different climatic and geological conditions, but also of building regulations.

This paper aims to put Romania on the map of research centers in Europe where the coupling of geothermal HP systems together with energy efficient buildings are analyzed and studied intensively with the aim of promoting the benefits of implementing this system, reducing energy consumption and CO_2 emissions.

The elaborated doctoral thesis extends over 203 pages, containing an introductory chapter, two chapters of documentary synthesis with novel aspects and some contributions in the field, four consistent chapters related to the research problem and a final chapter that includes final

conclusions, personal contributions and new research directions. The scientific approach is accompanied by 124 figures, 52 tables, 131 formulas, as well as 185 appropriate, recent bibliographic references. The way to achieve the main objective is demonstrated by the structure of the thesis and the content of each of its chapters.

2. HEAT PUMP WITH ELECTROCOMPRESSOR

Chapter 2 discusses HP systems with mechanical vapor compression, describing the operating principle (Fig. 2.1), the theoretical thermodynamic cycle of the subcooled and liquid separator plant, the actual cycle of the standard plant, as well as their calculation. Also, the calculation of the energy and economic performance indicators that allow the implementation of a HP in a heating/cooling system and its GHG emissions are considered and the main natural heat sources (air, water, soil) are presented) and types of HP.

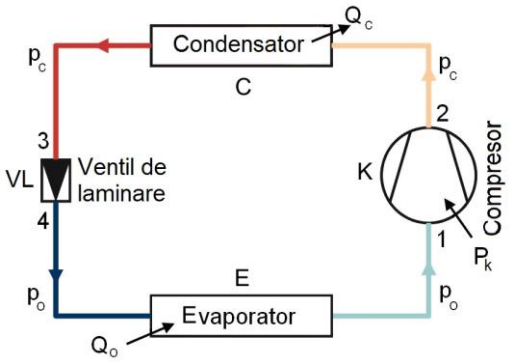

Fig. 2.1 Functional scheme of a heat pump

The HP incorporates four main components: the compressor (K), the evaporator (E), the condenser (C) and an expansion valve (VL). The main auxiliary components are fans, pipes, measuring and control devices. Fig. 2.1 shows the basic schematic of mechanical vapor compression HP, with the most common thermodynamic cycle configuration.

HP for heating works according to the following steps [10]:

1. In E, the liquid refrigerant extracts heat from a heat source and evaporates. After the evaporator refrigerant is in the low-pressure vapor state, the temperature rises slightly.

2. Refrigerant in vapor state flows in electric K; here the pressure is increased, resulting in an increase in temperature.

3. Heat transfer to the building's heating system causes the refrigerant to cool and condense into liquid C at high pressure and temperature.

4. The warm liquid passes through a VL, where its pressure is reduced, in turn lowering its temperature. The refrigerant returns to the evaporator and the cycle repeats.

The feasibility of implementing a PC in a heating/cooling system is based on various energy indicators and an economic analysis.

• *The performance coefficient* (COP_{HP}) of HP represents the ratio between the useful thermal energy E_t and the electrical energy E_{el} absorbed by the compressor [10]:

$$COP_{HP} = \frac{E_t}{E_{el}} \tag{2.15}$$

If, in Eq. (2.15), thermal energy and electrical energy are added up during the operating period (month, season, year), the seasonal performance coefficient (COP_{ses}), often referred to as seasonal performance factor (SPF) or annual efficiency, is obtained.

In the case of a reversible HP (heating-cooling), the COPHP in heating mode is defined by the relationship:

$$\mathrm{COP_{HP}} = \frac{Q_{\mathrm{HP}}}{P_{\mathrm{e}}} \tag{2.16}$$

where Q_{HP} is the HP heating power, in W, and P_e is the electrical power to drive the compressor, in W.

The energy efficiency ratio EER_{HP}, in Btu/(h·W), of a HP in cooling mode is given by the relationship:

$$\mathrm{EER_{HP}} = \frac{Q_0}{P_{\mathrm{e}}} \tag{2.17}$$

and the corresponding COP_{HP} yields:

$$\mathrm{COP_{HP}} = \frac{\mathrm{EER_{HP}}}{3,412} \tag{2.18}$$

where: Q_0 is the HP cooling capacity, in Btu/h; P_e is the electrical power absorbed by the compressor, in W; and 3.412 is the conversion factor of W in Btu/h.

The performance coefficient of the entire system, COP_{syst} is given by the relationship [11]:

$$\mathrm{COP}_{syst} = \frac{Q_{\mathrm{HP}}}{P_{\mathrm{e}} + P_{\mathrm{aux}}} \tag{2.20}$$

where: Q_{HP} is the HP heating capacity, in W; P_e is the electrical driving power of the compressor, in W; P_{aux} is the electrical power consumed by the auxiliary equipment of the system (pumps, fans, etc.).

- *The economic analysis* of a system uses different evaluation methods. Some of them are: present cost method (PC), total annual cost method (TAC), total updated cost method (TUC), payback (recovery) time method (RT).

Present cost analysis. The PC of a future payment can be calculated using Eq. (2.30) [12]:

$$\mathrm{PC} = u_r \mathrm{TAC} \tag{2.30}$$

with:

$$u_r = \frac{(1+\beta_0)^{\tau} - 1}{\beta_0 (1+\beta_0)^{\tau}} \tag{2.31}$$

where: TAC is the total annual cost (sum of all annual costs of each system component); τ is the number of periods (years); u_r is the update (discount) rate; β_0 is the average inflation rate.

Total updated cost TUC are expressed by the Eq. (2.32) [13]:

$$\mathrm{TUC} = I_0 + u_{\mathrm{r}} C_{ex} \tag{2.32}$$

in which: I_0 is the initial investment cost, and C_{ex} is the annual operation and maintenance cost of the system.

The payback time RT, in years, of the additional investment ΔI, due to the reduction of the operating cost ΔC_{ex} can be determined as follows [10]:

$$\mathrm{RT} = \frac{\Delta I}{\Delta C_{ex}} \leq \mathrm{RT}_n \tag{2.33}$$

where TR is the normed recovery time, with an acceptable value of 8–10 years.

• *The carbon dioxide emission* M_{CO_2}, in kg, of a PC during its operation can be evaluated with the following relationship [1]:

$$M_{CO_2} = g_{el} E_{el} \tag{2.34}$$

where g_{el} is the specific CO_2 emission factor for electricity.

Natural heat sources are all the sources that can be found and used directly or indirectly from nature, including the exterior air, surface water (river, lake, sea) and underground water (phreatic, geothermal), soil and solar radiation, all having a temperature variation depending on the evolution of the seasons. In order to avoid the negative effect of the drop in exterior air temperature on the energy performance of the HP, it is recommended to interconnect it with an auxiliary heat source. Surface water is indicated as a heat source in special cases where, upstream of urban concentrations, there are industrial enterprises that use river water for cooling processes in open circuit. The most important advantage of using soil in HPs is that the heat source is almost completely independent of heat demand and has no minimum capacity in the middle of the cold season, unlike other natural sources.

HPs can be classified according to:

– purpose of use: heating, cooling, DHW, air conditioning, etc.

– heat source: air, surface water, underground water, soil, etc.

– heat source-thermal agent: air-air, air-water, water-air, air-water, water-water, soil-water.

It also presents an extensive documentary synthesis with novel aspects, regarding the impact of refrigerants on the environment and the recent development of possible substitutes for non-ecological refrigerants in HP equipment based on thermodynamic, physical and environmental properties and total equivalent warming impact (TEWI), also showing the influence of refrigerants on the efficiency of the refrigeration cycle. Finally, a study of the effectiveness of refrigerants on the coefficient of performance of HP (COP_{HP}) is carried out, proposing a simple and fast method for calculating COP_{HP} based on the vaporization and condensation temperatures of the refrigerant used and the Jacob number, which includes the specific heat of the liquid refrigerant and the latent heat of condensation.

The *Z*-inefficiency approach of a refrigerant has been developed for rapid evaluation of HP system thermal efficiency with only operating temperature values. Thus, the thermodynamic properties of several refrigerants have been set as a dimensional group called inefficiency (*Z*), which includes specific heat and latent heat of vaporization in the form of the Jacob number (Ja), vaporization temperature, and condensation temperature. A correlation in the form of a Lagrange polynomial was established between the COP_{HP} of the HP standard cycle and *Z*:

$$COP_{HP} = 328.19Z^2 - 140.22Z + 18.366 \tag{2.42}$$

where:

$$Z = Ja^{0.1}\frac{T_c - T_0}{T_c}; \quad \text{Ja} = \frac{c_p \Delta T}{r} \tag{2.43}$$

in which: Ja is the Jacob number; T_c is absolute condensation temperature, in K; T_0 is the absolute vaporization temperature, in K; c_p is the specific heat of the liquid at the average temperature between vaporization and condensation, in kJ/(kgK); ΔT is the difference between the vaporization temperature and the condensation temperature, in °C; r is the latent heat of condensation, in kJ/kg.

For the validation of the Z model, the experimental data from the literature were compared with the COP values calculated from the developed correlation. The deviation between the Z model and the experimental data was determined by the mean absolute relative error with acceptable values below 7%.

The COP_{HP}–Z correlation for R-410A, with which the experimental laboratory HP operates, is evaluated at various condensing temperatures in the range 35–65 °C and vaporization temperatures between −10 °C and +5 °C. The performance coefficient decreases with increasing inefficiency (*Z*), respectively with decreasing efficiency (1/*Z*) of the refrigerant.

3. GEOTHERMAL HEAT PUMPS

Chapter 3 presents a brief description of Geothermal HP (GHP), focusing on Ground-Coupled HP (GCHP), where heat is extracted/injected into/from the ground through a ground-mounted heat exchanger (GHE), horizontally or vertical, with U-tubes, usually made of high-density polyethylene (HDPE). The main numerical and analytical models for simulating vertical GHE both inside and outside the borehole are summarized and some of their design/ simulation programs are briefly described. Additionally, a transient heat transfer simulation model between vertical GHE and soil in both double and single U-tube configurations is formulated, which can be solved by numerical finite difference method. Finally, a theoretical study on closed-loop GCHP with vertical GHEs combined with solar collectors is carried out and a new performance indicator SPF_{HP-PV} (global seasonal performance factor), which includes subsystem integration (HP and PV generator) and the renewable nature of HP-PV.

GHP technology has become increasingly popular due to its efficiency, environmental compatibility and its potential to retrofit buildings without replacing existing radiators. A reduction in building energy demand of 20–40% for heating and 30–50% for cooling, respectively, could be achieved with GHPs, along with a reduction in CO_2 emissions of 15% to 77%, considering both residential and non-residential buildings [14].

GHPs inject (in the cooling season) or extract (in the heating season) heat through a GHE and can be grouped into three subsets (Fig. 3.1):

- Surface water source HP (SWHP) (water-water type);
- Groundwater source HP (GWHP) (water-water type);
- Ground-coupled HP (GCHP) (soil-water type).

A SWHP system extracts/injects heat from/into water in a lake, pond or open canal using the working fluid, which circulates through HDPE pipes. A GWHP system draws groundwater from an extraction well using hydraulic pumps and delivers it to a HP.

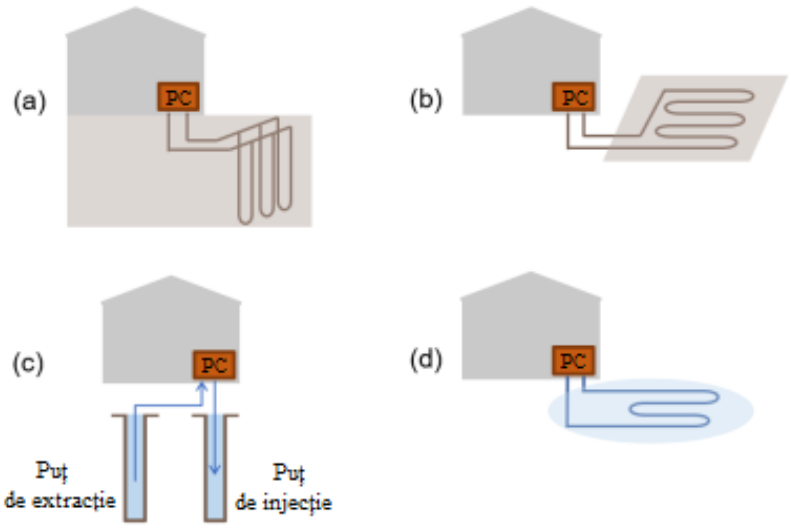

Fig. 3.1 Scheme of the main types of geothermal heat pumps
(a) vertical GCHP; (b) horizontal GCHP; (c) GWHP; d) SWHP

The GCHP system consists of a reversible refrigerant vapor compression cycle in which heat is exchanged with the ground through the GHE, a closed circuit with the working fluid (ethylene glycol solution), which can be installed either in vertical boreholes or in horizontal trenches. Based on the spatial arrangement, GHEs can be divided into two broad categories, horizontal ground heat exchangers (HGHE) and vertical ground heat exchangers (VGHE) (Fig. 3.4), in U-tube or concentric (coaxial) tube configuration (Fig. 3.7). The annular space (free between the borehole walls and the tube) of the drilled well is filled with a special material called grout to prevent direct contact with water.

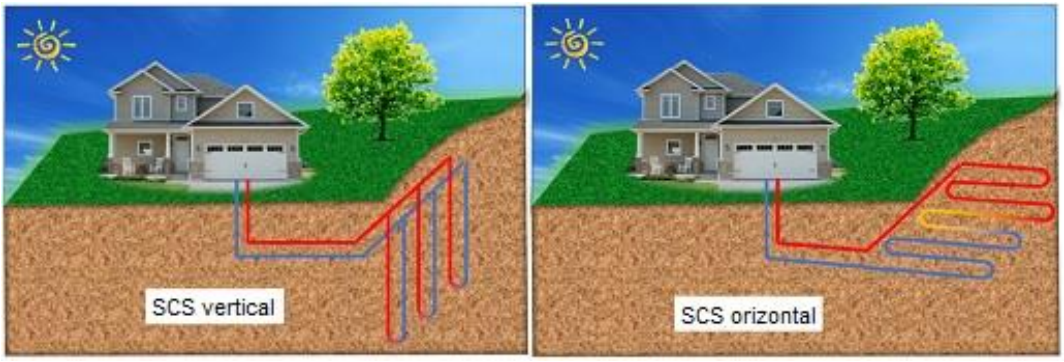

Fig. 3.4 Vertical and horizontal GHE configuration

Fig. 3.7 Models of vertical ground heat exchangers

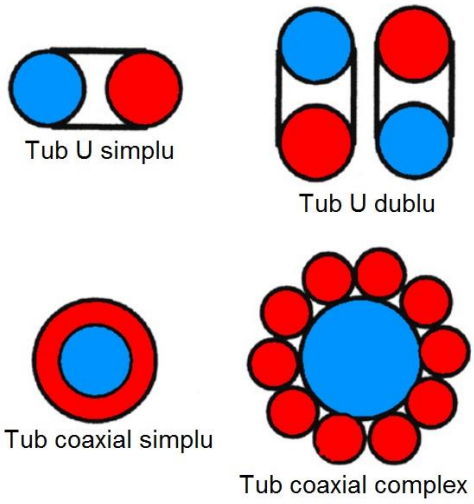

The vertical PCCS system requires relatively little land area, is in contact with the ground, which has small variations in temperature and thermal properties, and requires little piping and pumping energy, but has a high cost due to the equipment required to drill the well.

Several analytical and numerical models have been developed to obtain the transient heat transfer from the outside of the borehole, but also some mathematical models to describe the heat transfer inside the borehole. Table 3.4 presents a summary of the main vertical GHE models. Computer-aided simulation tools are also available for heat transfer analysis of horizontal GHEs with various configurations [15].

For vertical GHEs, a series of design programs have been developed in the last two decades, based on typical heat transfer models, such as the linear source model: the *EED*, *GLHEPRO* and *GEOSTAR* programs, the cylindrical source model: the *GCHPCalc* program and numerical simulation programs: *EnergyPlus*, *eQUEST* and *TRNSYS*.

Table 3.4 Vertical GHE models

Region	Model	Equation	Reference
GHE exterior	Infinite linear source	$t(r,\tau)-t_0=\frac{q}{4\pi\lambda_s}\int_{\frac{r^2}{4a_s\tau}}^{\infty}\frac{e^{-u}}{u}du=\frac{q}{4\pi\lambda_s}\left(\ln\frac{4a_s\tau}{r_p^2}-\gamma\right)$	Kelvin [16]
	Cylindrical source	$t-t_0=\frac{q}{\lambda_s}G(z,p)$	Carslaw and Jaeger [17]
	Eskilson	$t_p-t_0=-\frac{q}{2\pi\lambda_s}f(\tau/\tau_s,r_p/L)$	Eskilson [18]
GHE interior	Empirical	$R_p=\frac{1}{\beta_0\left(r_p/r_t\right)^{\beta_1}\lambda_g}$	Paul [19]
	Linear source	$R_p=\frac{1}{4\pi\lambda_g}\left(\ln\frac{r_p}{r_t}+\ln\frac{r_p}{2x_c}+\frac{\lambda_g-\lambda_s}{\lambda_g+\lambda_s}\ln\frac{(r_p/x_c)^4}{(r_p/x_c)^4-1}\right)$	Pahud et al. [20]
	2D finite element simulations	$R_p=\frac{1}{4\pi\lambda_g}\left(-1,49\ln\frac{r_p}{x_c}+0,656\ln\frac{r_p}{r_t}+0,436\right)$	Sharqawy et al. [21]

To account for the actual transient heat transfer between the vertical GHE and the ground, in both double and single U-tube configurations, allowing performance comparison between the two GHEs for injection or extraction mode of operation of heat, *a numerical simulation model of the transient heat transfer* between the GHE and the soil was formulated.

The heat transfer mechanism in GHE consists of convection between the working fluid and the tube wall, and conduction between the tube wall and the grout, as well as between the grout and the soil. The numerical model developed for the double U-tube borehole [22] has been modified to also allow the simulation of the single U-tube GHE. The differential heat transfer equations are obtained by writing the energy balance for the fluid, grout and soil, and are then discretized to be solved at each time step by the Crank-Nicolson finite difference numerical method, using the MATLAB or FORTRAN programming environment.

Fig. 3.13 illustrates the sectional view of the double U-tube GHE configuration and the borehole geometric parameters. The tubes are considered symmetrically placed in the borehole with two independent circuits 1–3 and 2–4, adopted based on the results of the study carried out by Zeng et al. [23].

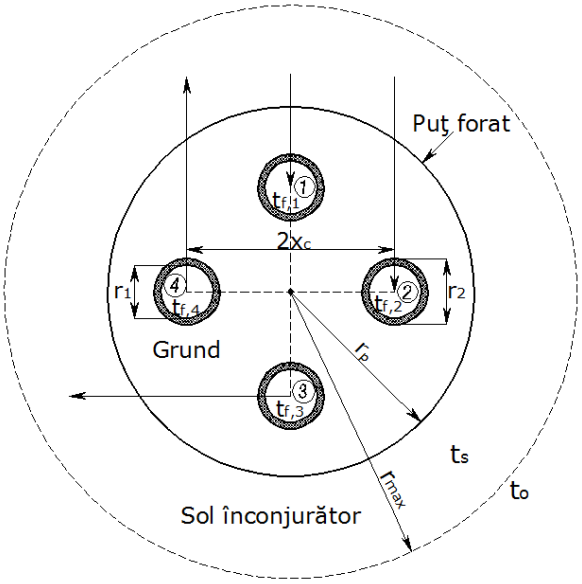

Fig. 3.13 Borehole geometric parameters and double U-tube GHE configuration

The set of differential equations with respect to time τ governing the heat transfer inside the double U-tube borehole is obtained from the energy balance equations for fluid in tube 1, 3, 2, 4, respectively, and grout written using nodes *i* at the borehole depth, taking into account the Crank-Nicolson equation [24] and conveniently rearranged as follows:

$$
\begin{aligned}
&-\frac{\Delta\tau\times m_f}{2M_f}t_{f1,i-1}^{j+1}+\left[1+\frac{\Delta\tau}{2}\left(\frac{1}{M_fc_fR_{12}^{\Delta}/\Delta z}+\frac{1}{M_fc_fR_{13}^{\Delta}/\Delta z}+\frac{1}{M_fc_fR_{14}^{\Delta}/\Delta z}+\frac{1}{M_fc_fR_{fg}/\Delta z}+\frac{m_f}{M_f}\right)\right]t_{f1,i}^{j+1}\\
&=\frac{\Delta\tau\times m_f}{2M_f}t_{f1,i-1}^{j}+\left[1-\frac{\Delta\tau}{2}\left(\frac{1}{M_fc_fR_{12}^{\Delta}/\Delta z}+\frac{1}{M_fc_fR_{13}^{\Delta}/\Delta z}+\frac{1}{M_fc_fR_{14}^{\Delta}/\Delta z}+\frac{1}{M_fc_fR_{fg}/\Delta z}+\frac{m_f}{M_f}\right)\right]t_{f1,i}^{j}\\
&+\frac{\Delta\tau}{M_fc_fR_{12}^{\Delta}/\Delta z}t_{f2,i}^{j}+\frac{\Delta\tau}{M_fc_fR_{13}^{\Delta}/\Delta z}t_{f3,i}^{j}+\frac{\Delta\tau}{M_fc_fR_{14}^{\Delta}/\Delta z}t_{f4,i}^{j}+\frac{\Delta\tau}{M_fc_fR_{fg}/\Delta z}t_{g,i}^{j}
\end{aligned}
\tag{3.27}
$$

$$
\begin{aligned}
&\left[1+\frac{\Delta\tau}{2}\left(\frac{1}{M_fc_fR_{13}^{\Delta}/\Delta z}+\frac{1}{M_fc_fR_{23}^{\Delta}/\Delta z}+\frac{1}{M_fc_fR_{34}^{\Delta}/\Delta z}+\frac{1}{M_fc_fR_{fg}/\Delta z}+\frac{m_f}{M_f}\right)\right]t_{f3,i}^{j+1}-\frac{\Delta\tau\times m_f}{2M_f}t_{f3,i+1}^{j+1}\\
&=\left[1-\frac{\Delta\tau}{2}\left(\frac{1}{M_fc_fR_{13}^{\Delta}/\Delta z}+\frac{1}{M_fc_fR_{23}^{\Delta}/\Delta z}+\frac{1}{M_fc_fR_{34}^{\Delta}/\Delta z}+\frac{1}{M_fc_fR_{fg}/\Delta z}+\frac{m_f}{M_f}\right)\right]t_{f3,i}^{j}+\frac{\Delta\tau\times m_f}{2M_f}t_{f3,i+1}^{j}\\
&+\frac{\Delta\tau}{M_fc_fR_{13}^{\Delta}/\Delta z}t_{f1,i}^{j}+\frac{\Delta\tau}{M_fc_fR_{23}^{\Delta}/\Delta z}t_{f2,i}^{j}+\frac{\Delta\tau}{M_fc_fR_{34}^{\Delta}/\Delta z}t_{f4,i}^{j}+\frac{\Delta\tau}{M_fc_fR_{fg}/\Delta z}t_{g,i}^{j}
\end{aligned}
\tag{3.28}
$$

$$
\begin{aligned}
&-\frac{\Delta\tau\times m_f}{2M_f}t_{f2,i-1}^{j+1}+\left[1+\frac{\Delta\tau}{2}\left(\frac{1}{M_fc_fR_{12}^{\Delta}/\Delta z}+\frac{1}{M_fc_fR_{23}^{\Delta}/\Delta z}+\frac{1}{M_fc_fR_{24}^{\Delta}/\Delta z}+\frac{1}{M_fc_fR_{fg}/\Delta z}+\frac{m_f}{M_f}\right)\right]t_{f2,i}^{j+1}\\
&=\frac{\Delta\tau\times m_f}{2M_f}t_{f2,i-1}^{j}+\left[1-\frac{\Delta\tau}{2}\left(\frac{1}{M_fc_fR_{12}^{\Delta}/\Delta z}+\frac{1}{M_fc_fR_{23}^{\Delta}/\Delta z}+\frac{1}{M_fc_fR_{24}^{\Delta}/\Delta z}+\frac{1}{M_fc_fR_{fg}/\Delta z}+\frac{m_f}{M_f}\right)\right]t_{f2,i}^{j}\\
&+\frac{\Delta\tau}{M_fc_fR_{12}^{\Delta}/\Delta z}t_{f3,i}^{j}+\frac{\Delta\tau}{M_fc_fR_{23}^{\Delta}/\Delta z}t_{f3,i}^{j}+\frac{\Delta\tau}{M_fc_fR_{24}^{\Delta}/\Delta z}t_{f4,i}^{j}+\frac{\Delta\tau}{M_fc_fR_{fg}/\Delta z}t_{g,i}^{j}
\end{aligned}
\tag{3.29}
$$

$$
\begin{aligned}
&\left[1+\frac{\Delta\tau}{2}\left(\frac{1}{M_fc_fR_{14}^{\Delta}/\Delta z}+\frac{1}{M_fc_fR_{24}^{\Delta}/\Delta z}+\frac{1}{M_fc_fR_{34}^{\Delta}/\Delta z}+\frac{1}{M_fc_fR_{fg}/\Delta z}+\frac{m_f}{M_f}\right)\right]t_{f4,i}^{j+1}-\frac{\Delta\tau\times m_f}{2M_f}t_{f4,i+1}^{j+1}\\
&=\left[1-\frac{\Delta\tau}{2}\left(\frac{1}{M_fc_fR_{14}^{\Delta}/\Delta z}+\frac{1}{M_fc_fR_{24}^{\Delta}/\Delta z}+\frac{1}{M_fc_fR_{34}^{\Delta}/\Delta z}+\frac{1}{M_fc_fR_{fg}/\Delta z}+\frac{m_f}{M_f}\right)\right]t_{f4,i}^{j}+\frac{\Delta\tau\times m_f}{2M_f}t_{f4,i+1}^{j}\\
&+\frac{\Delta\tau}{M_fc_fR_{14}^{\Delta}/\Delta z}t_{f1,i}^{j}+\frac{\Delta\tau}{M_fc_fR_{24}^{\Delta}/\Delta z}t_{f2,i}^{j}+\frac{\Delta\tau}{M_fc_fR_{34}^{\Delta}/\Delta z}t_{f3,i}^{j}+\frac{\Delta\tau}{M_fc_fR_{fg}/\Delta z}t_{g,i}^{j}
\end{aligned}
\tag{3.30}
$$

$$
\begin{aligned}
&\left[1+\frac{\Delta\tau}{2}\left(\frac{4}{R_{fg}/M_gc_g\Delta z}+\frac{1}{R_{gp}/M_gc_g\Delta z}\right)\right]t_{g,i}^{j+1}=\left[1-\frac{\Delta\tau}{2}\left(\frac{4}{R_{fg}/M_gc_g\Delta z}+\frac{1}{R_{gp}/M_gc_g\Delta z}\right)\right]t_{g,i}^{j}+\\
&\frac{\Delta\tau}{R_{fg}/M_gc_g\Delta z}\left(t_{f1,i}^{j}+t_{f2,i}^{j}+t_{f3,i}^{j}+t_{f4,i}^{j}\right)+\frac{\Delta\tau}{R_{gp}/M_gc_g\Delta z}t_{p,i}^{j}
\end{aligned}
\tag{3.31}
$$

The Crank-Nicolson equations for soil nodes outside the borehole defined by the index *i* in the vertical direction and *k* in the radial direction are of the form:

$$-\frac{\Delta\tau}{2M_{s,k}c_sR_{s,k}/\Delta z}t_{s,(i,k-1)}^{j+1}+\left[1+\frac{\Delta\tau}{2}\left(\frac{1}{M_{s,k}c_sR_{s,k}/\Delta z}+\frac{1}{M_{s,k}c_sR_{s,k+1}/\Delta z}\right)\right]t_{s,(i,k)}^{j+1}-\frac{\Delta\tau}{2M_{s,k}c_sR_{s,k+1}/\Delta z}t_{s,(i,k+1)}^{j+1}$$
$$=\frac{\Delta\tau}{2M_{s,k}c_sR_{s,k}/\Delta z}t_{s,(i,k-1)}^{j}+\left[1-\frac{\Delta\tau}{2}\left(\frac{1}{M_{s,k}c_sR_{s,k}/\Delta z}+\frac{1}{M_{s,k}c_sR_{s,k+1}/\Delta z}\right)\right]t_{s,(i,k)}^{j}+\frac{\Delta\tau}{2M_{s,k}c_sR_{s,k+1}/\Delta z}t_{s,(i,k+1)}^{j} \quad (3.32)$$
$$(i=1,2,...,N;\quad k=1,2,...,n)$$

where: m_f is the fluid mass flow rate, in kg/s; $\Delta\tau$ is the time step, in s; t_f is the fluid temperature, in °C; $M_f=\rho_f\pi r_1^2Z$ is the fluid mass, in kg; ρ_f is the fluid density, in kg/m^3; Z is the borehole depth, in m; ; c_f is the specific heat of the fluid, in W/(m^{2}K); Δz is the vertical distance between adjacent nodes (depth step), in m; t_g is the grout temperature, in °C; R_{fg} is the thermal resistance between fluid and grout, in m·K/W; $M_g=\rho_g\pi\left(r_p^2-4r_2^2\right)Z$ is the mass of the grout, in kg, in the case of the double U-tube, which becomes $M_g=\rho_g\pi\left(r_p^2-2r_2^2\right)Z$ in the case of the single-U tube; ρ_g is the density of the grout; R_{gp} is the thermal resistance between soil and borehole, in m·K/W; t_p is the borehole wall temperature, in °C; $M_{s,k}=\rho_s\pi\left(r_k^2-r_p^2\right)Z$ is the mass of soil in node k, in kg; ρ_s is the soil density; $r_k = k\Delta r$ is the distance in the radial direction from the center of the borehole to the soil node k, in m; Δr is the radial step, in m; $R_{s,k}=2r_k/\left[\lambda_s\pi\left(r_k^2-r_p^2\right)\right]$ is the linear thermal resistance of the soil in node k, in m·K/W; λ_s is the thermal conductivity of the soil, in W/(m·K); t_s is the soil temperature.

Equations (3.27) – (3.32), except equations (3.29) and (3.30), are also the heat transfer modeling equations for the vertical GHE in simple U-tube configuration.

Solar powered GCHP systems are systems connected to PV panels, where solar energy is initially converted into electricity and then used to drive the HP. Fig. 3.21 shows the scheme of a hybrid HP-PV system with direct vaporization [25]. The electricity $E_{el,pv}$ produced by the PV generator (GPV) is used to power the compressor and other auxiliary consumers with an inverter and a battery, in a stand-alone configuration, or combined with the power grid, in a grid-connected configuration.

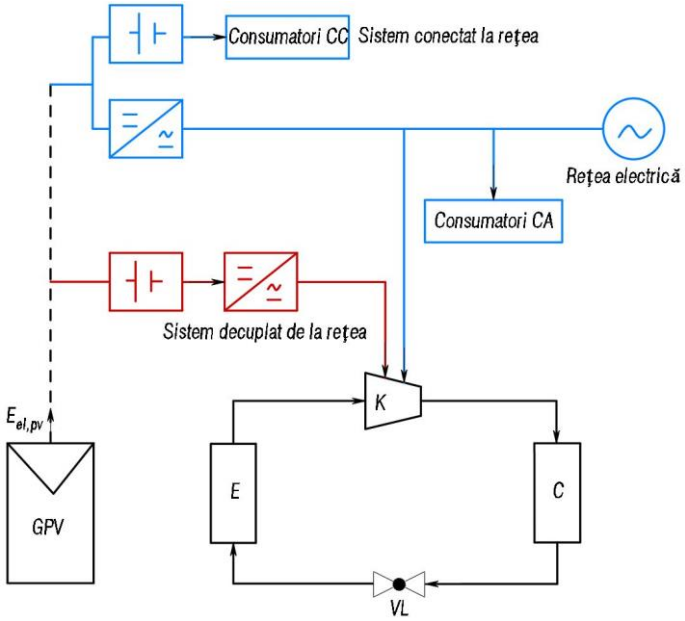

Fig. 3.21 Scheme of a hybrid HP-PV system

For hybrid HP-PV systems, there are three energy performance indicators commonly used to evaluate the PV contribution: the solar fraction photovoltaic (SF_{PV}) to evaluate the quality of the connection between the GPV and the compressor, the performance ratio (PR_{PV}) of the GPV and the self-consumption ratio (SCR).

A combination of the previously mentioned indicators helps to integrate three different characteristics of the hybrid HP-PV system to be evaluated: HP quality (characterized by COP_{HP}, EER_{HP} and/or SPF_{HP}), GPV quality (characterized by RP_{PV}) and quality of the integration of the two subsystems (characterized by SCR and SF_{PV}).

That is why a new seasonal performance factor (SPF_{HP-PV}) is introduced, specific to hybrid HP-PV systems, resulting from the combination of SPF_{HP}, PR_{PV}, SCR and SF_{PV} indicators:

$$SPF_{HP-PV} = SPF_{HP}\left(1 + PR_{PV} \times SCR \times SF_{PV}\right) \tag{3.63}$$

where SPF_{HP-PV} and SPF_{HP} can be extended to different periods (hourly, monthly, yearly).

In this way, the SPF_{HP-PV} can be considered as an indicator of the performance of the entire hybrid system, including the integration of the two subsystems (HP and GPV) and the renewable nature of the HP-PV. A high SPF_{HP-PV} value means a high HP efficiency, an efficient use of PV electricity and therefore a good integration of both subsystems.

In the case of constructions with a dominant heating demand, the interconnection of the GCHP with an ST collector or a PV/T panel can significantly reduce the length of the GHE and therefore its cost.

4. EXPERIMENTAL LABORATORY

Chapter 4 refers to the experimental laboratory (the space of an office), for which a brief description is performed and the structure and characteristics of the building elements are presented, as well as the climatic conditions specific to the site, as well as the theoretical aspects regarding the calculation of the thermal power of heating, cooling and production of DHW, according to the current legislation.

The laboratory for the experimental studies of the energy and environmental performances of a closed-loop GCHP consists of an office space located on the ground floor of the building of the Faculty of Civil Engineering in Timisoara (Fig. 4.1) equipped with four heating systems (floor, wall and ceiling radiant panels and medium temperature radiators).

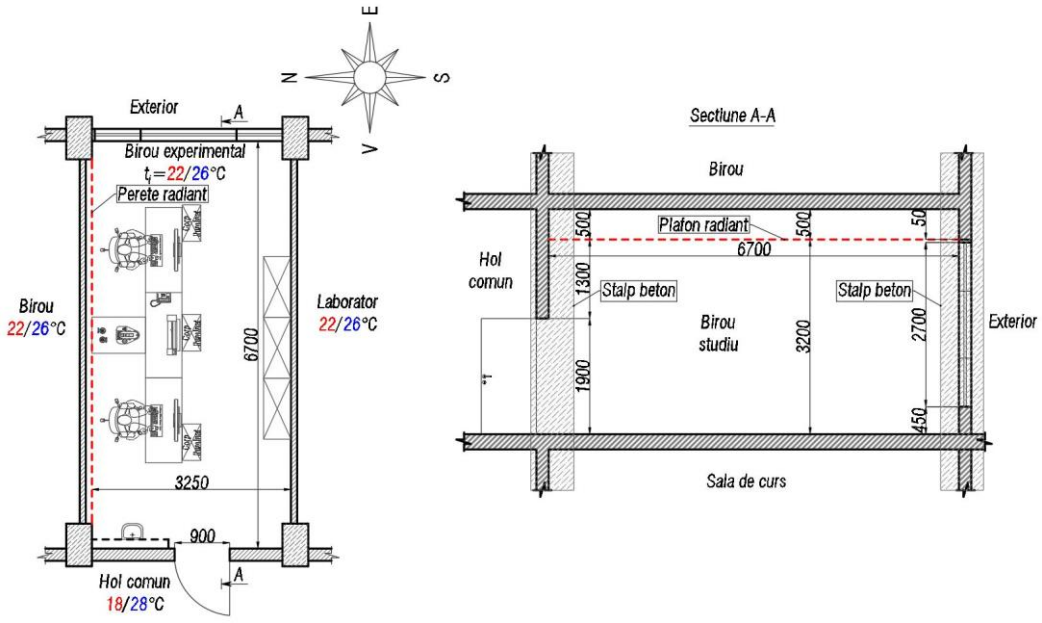

Fig. 4.1 Heated/cooled office space

The heating thermal power $Q_{înc}$, in W, was determined according to the SR 1907/1-2014 standard [26], and the cooling thermal power was calculated according to the SR 6648/1-2014 standard [27], the results being summarized in Tables 4.5 and 4.6.

Table 4.5 Calculation of the heating thermal power for office

Room	Elem	Or.	Width (m)	Height (m)	Area (m^2)	S_{gol} (m^2)	A_j (m^2)	R'_j (m^2K/W)	t_i (°C)	$t_{e,j}$ (°C)	c_M (–)	Q_T (W)	V_i (m^3)	n_a (h^{-1})	Q_{inf} (W)	$Q_{înc}$ (W)
Office	PE	E	3,25	3,2	10,4	8,20	2,20	1,18	22	–15	1	69,0	69,7	0,8	695,5	**1182**
	FE	E	3,04	2,7	8,20		8,20	0,77		–15	1	394				
	PI	S	6,70	3,2	21,4		21,4	2,67		22	1	0				
	PI	V	3,25	3,2	10,4	1,71	8,69	2,67		18	1	13,0				
	UI	V	0,90	1,9	1,71		1,71	0,65		18	1	10,5				
	PI	N	6,70	3,2	21,4		21,4	2,67		22	1	0				
	PA	–	3,25	6,7	21,8		21,8	0,34		22	1	0				
	PL	–	3,25	6,7	21,8		21,8	0,34		22	1	0				
											Total	486,5				

Table 4.6 Calculation of the cooling thermal power for office

Hour	Exterior air temperature (°C)	Heat inputs				Heat releases	$Q_{răc}$ (W)
		$Q_{PE, EST}$ (W)	$Q_{FE, EST}$ (W)	$Q_{PI, EST}$ (W)	Q_{ap} (W)	Q_{deg} (W)	
1	24,6	–2,6		–4,8	–7,4	316,4	**969**
2	23,5	–4,7		–1,9	–22,5		
3	23,1	–5,4		–22,6	–28,0		
4	22,3	–6,9		–32,2	–39,1		
5	21,8	–7,8		–38,1	–45,9		
6	21,5	–8,4	710,4	–41,7	360,3		
7	20,7	–9,9	518,9	–51,2	457,8		
8	20,8	–9,7	612,3	–50,0	552,6		
9	21,7	–8,0	666,7	–39,3	619,4		
10	23,9	–3,9	669,6	–13,1	652,6		
11	26,8	1,5	584,2	21,4	607,1		
12	29,7	6,9	117,1	56,0	179,9		
13	33,1	13,2	101,3	96,5	211,0		
14	35,0	16,8	87,7	107,2	211,7		
15	36,5	19,6	74,2	125,1	218,8		
16	36,9	20,3	65,2	129,8	215,3		
17	37,7	21,8	58,4	139,3	219,6		
18	38,5	23,3	51,6	148,9	223,8		
19	37,8	22,0		140,5	162,5		
20	38,0	22,4		142,9	165,3		
21	37,1	20,7		132,2	152,9		
22	33,0	13,1		83,4	96,4		
23	28,2	4,1		26,2	30,3		
24	27,2	2,2		14,3	16,5		
				Maximum value	652,6		

The thermal energy consumed monthly to satisfy the heating and cooling power of the experimental office was determined according to the norm NP 048-2000 [28], and respectively the methodology Mc 001/4-2006 [29] and was represented graphically in Fig. 4.6. The hourly energy consumption for the production of DHW was also calculated, according to the Mc 001/2-2006 methodology [30], in the case of three different temperatures (45, 50, 55 °C), and represented graphically beside the values obtained from the measurements.

The obtained results were later used in the choice of equipment and the dimensioning of the heating/cooling system.

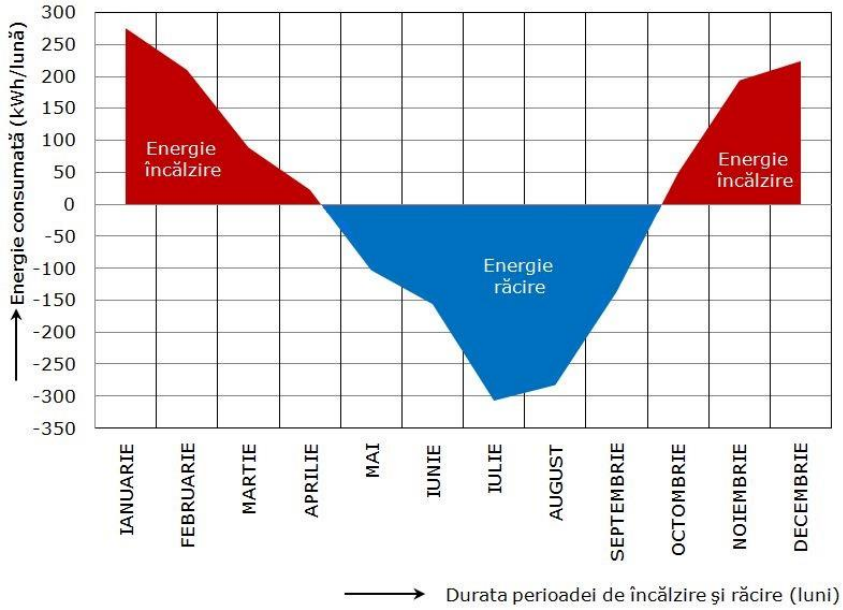

Fig. 4.6 Monthly thermal energy consumption for office heating and cooling

5. STUDIES AND EXPERIMENTAL INVESTIGATIONS ON THE BEHAVIOR OF THE GROUND-COUPLED HEAT PUMP

Chapter 5 includes an essential part of the thesis, being focused in the first part on the energy and environmental analysis of the experimental geothermal system (Fig. 5.1).

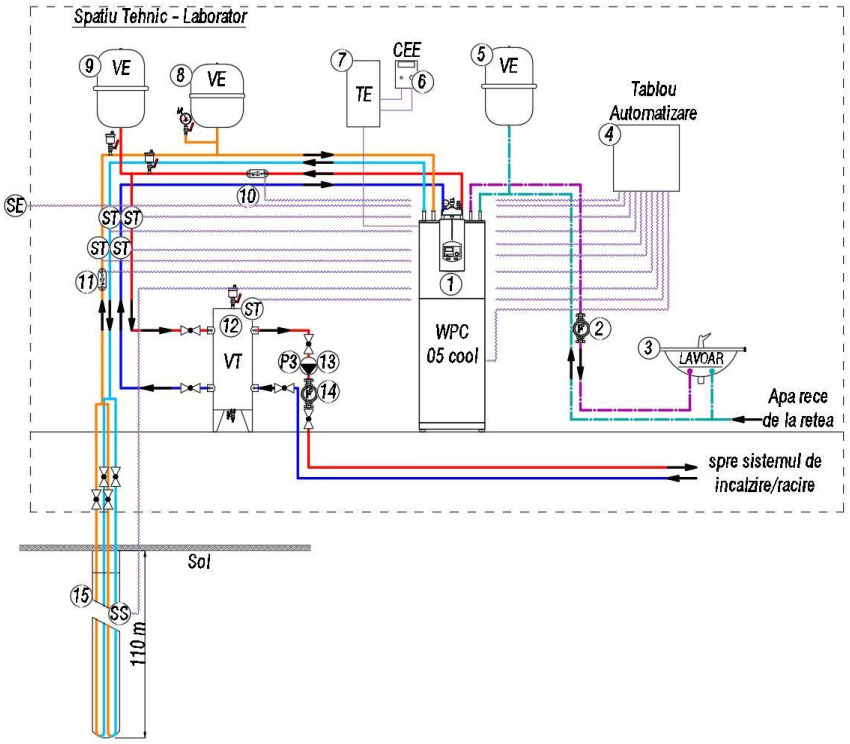

Fig. 5.1 Scheme of the experimental GCHP facility

1-GCHP; 2-DHW meter; 3-sink; 4-automation panel; 5-DHW expansion tank; 6-three-phase electronic electricity meter; 7-electrical distribution panel of the stand; 8-expansion tank of the GHE circuit; 9-expansion tank of the heating/cooling circuit; 10-flowmeter for the heating/cooling circuit; 11-ultrasonic flowmeter for the GHE circuit; 12- buffer tank; 13-circulation pump of the heating/cooling circuit (P3); 14-flow meter with turbine; 15-double U-tube GHE; ST-temperature sensors; SS-temperature sensors mounted in the ground; SE-exterior air temperature sensor

The experimental system consists of a reversible vertical GCHP with hermetic scroll compressor and a single and double U-tube borehole with a heating capacity of 5.8 kW and a cooling capacity of 3.8 kW. Vertical GHE made of PE100-RC tubes, Ø32 x 2.9 mm, PN16, SDR11, coaxial type in double U construction, through which the heat transfer is carried out, is inserted into a borehole with a depth of 110 m and the exterior diameter of 180 mm and connected directly to the PC. The double U-tube borehole can be converted to a single U-tube borehole by sectoring with the help of shut-off valves. The cooling circuit of the HP is charged with refrigerant R410A. The thermal agent is delivered to 4 different heating/cooling circuits (radiant floor, radiant wall, radiant ceiling and medium temperature radiators).

The experimental facility contains 3 circulation pumps, two of which are mounted in the HP like this: one (P1) on the primary circuit (of the borehole) with a flow rate of 2.3 m^3/h and another (P2) on the secondary circuit between the HP and buffer tank/DHW, having a flow rate of 2.0 m^3/h, and the third (P3) on the secondary circuit between the buffer tank and the heating/cooling circuit, having a flow rate of 0.58 m^3/h. The operation of the P3 pump is independent of the operation of the other pumps in the HP. The main elements of the soil parameters monitoring system and HP are: temperature sensors, data acquisition modules, data logger and data computer.

To test the energy and environmental performance of the GCHP, a reference heating/ cooling system of the experimental office through the radiant floor composed of two circuits coupled to a manifold (D/C) was used, designed to cover the thermal power of experimental office heating and cooling of 1200 W and 969 W, respectively.

Thermal energy meters and three-phase electronic electricity meters were used to measure the amounts of energy (thermal and electrical) needed to calculate the energy performance (COP). The measurement of the temperature of the air, the heating agent and the working fluid was carried out with temperature sensors, and the measurement of the flow rates of DHW and heating agent was carried out with two flowmeters.

Experimental measurements are used to test the performance of the GCHP system in different operating modes. The main performance parameters (energy efficiency and CO_2 emission) were obtained for one month of operation using both double and single U-tube borehole. The average monthly values of the exterior air temperature (t_e) during the two periods were approximately equal. A comparative analysis of these performances is made for different operating modes: heating, heating–ACC, cooling, ACC, cooling–ACC, which are included in Tables 5.3–5.7.

Table 5.3 Performance of the GCHP system in heating mode

GHE configuration	t_i (°C)	t_e (°C)	t_f (°C)	E_t (kWh)	E_{el} (kWh)	COP_{syst}	COP_{PC}	M_{CO_2} (kg)
(1) Double U-tube	22.36	1.92	16.37	266.43	48.12	5.54	6.08	14.39
(2) Single U-tube	22.22	1.78	16.08	271.01	51.24	5.29	5.82	15.32

Table 5.4 Performance of the GCHP system in hybrid heating–DHW mode

GHE configuration	t_i (°C)	t_e (°C)	t_f (°C)	t_{dhw} (°C)	E_t (kWh)	E_{el} (kWh)	COP_{syst}	COP_{PC}	M_{CO_2} (kg)
(1) Double U-tube	22.36	–0.34	14.58	43.58	148.04	45.32	3.27	3.66	13.55
(2) Single U-tube	22.26	–0.14	14.95	43.66	146.96	46.86	3.14	3.56	14.01

Table 5.5 Performance of the GCHP system in cooling mode

GHE configuration	t_i (°C)	t_e (°C)	t_f (°C)	E_t (kWh)	E_{el} (kWh)	EER_{syst} (Btu/Wh)	COP_{syst}	M_{CO_2} (kg)
(1) Double U-tube	27.22	27.47	20.64	182.04	45.06	13.78	4.04	13.47
(2) Single U-tube	27.48	26.05	20.95	193.43	49.42	13.35	3.92	14.78

Table 5.6 Performance of the GCHP during DHW production tests

GHE configuration	$t_{dhw\text{-}set}$ (°C)	t_{dhw} (°C)	t_f (°C)	E_t (kWh)	E_{el} (kWh)	COP_{PC}	M_{CO_2} (kg)
1) Double U-tube	45	44.48	14.03	42.11	20.15	2.09	6.02
	50	49.39	13.89	48.10	24.41	1.97	7.30
	55	54.86	13.76	54.78	31.67	1.73	9.47
2) Single U-tube	45	44.56	14.79	41.36	19.58	2.11	5.85
	50	49.42	14.32	47.22	23.24	2.03	6.95
	55	54.72	14.08	53.79	29.94	1.80	8.95

Table 5.7 Performance of the GCHP system in combined cooling–DHW operating mode

GHE configuration	t_i (°C)	t_e (°C)	t_f (°C)	t_{dhw} (°C)	E_t (kWh)	E_{el} (kWh)	COP_{syst}	M_{CO_2} (kg)
(1) Double U-tube	26.82	29.28	17.48	43.51	104.42	28.61	3.66	8.55
(2) Single U-tube	26.94	28.33	17.81	43.64	101.21	30.04	3.37	8.98

The notations used in the tables are: t_i – indoor air temperature; t_f – working fluid temperature, t_{dhw} – DHW temperature; $t_{dhw\text{-}set}$ – reference DHW temperature, E_t – useful thermal energy; E_{el} – electrical energy consumed.

Experimental research has demonstrated higher performance of the GCHP system with double U-tube borehole compared to the single U-tube configuration (COP_{syst} increases by 3–8% and CO_2 emission decreases by 5–10%). The GCHP system operating in heating mode has a $COP_{syst} > 5$, and in cooling mode a $COP_{syst} \cong 4$, and the GCHP system operating in heating/cooling and DHW mode has a $3 < COP_{syst} < 4$, for both cases. The maximum error of the results was found to be for COP_{HP}, having an acceptable value of 1.3–1.4% in the heating mode and 1.0–1.1% in the cooling mode. The error for COP_{syst} was estimated to be 1.0–1.2% in heating mode and 1.1–1.3% in combined cooling-DHW mode.

A study is then carried out on the seasonal regeneration of GCHP by injecting and storing in the soil, during the summer season, thermal energy from an electrical resistance of a buffer tank, driven by electricity produced by 6 solar PV panels, before extracting the heat from the borehole for heating. For the heating system of the experimental office, with the radiant floor connected to the GCHP, it is found from the experimental results (Table 5.8) an increase in the average temperature of the working fluid by 2.4% and an improvement in the performance of the GCHP system in the case of using the injection of seasonal heat in both double and single U-tube borehole configuration (COP_{syst} 3.5% higher for single U-tube and 6.6% higher for double U-tube). After heat injection, there is also the highest increase in COP_{syst} in the double U-tube borehole configuration over the single U-tube, at 7.7%, and the highest reduction in CO_2 emissions at 6.9%. It was found that the maximum error of the results is for COP_{syst}, having an acceptable value of 1.8–2%.

Table 5.8 Performance of the GCHP system before and after heat injection into the soil

GHE configuration	t_i (°C)	t_e (°C)	t_f (°C)	E_t (kWh)	E_{el} (kWh)	COP_{syst} (–)	M_{CO_2} (kg)
Before heat injection							
(1) Double U-tube	22,28	–0,52	16,21	53,49	11,04	4,84	3,30
(2) Single U-tube	22,25	–0,47	15,56	53,28	11,51	4,63	3,44
After heat injection							
(1) Double U-tube	22,32	–0,27	16,60	54,86	10,63	5,16	3,18
(2) Single U-tube	22,26	–0,42	15,93	54,41	11,37	4,79	3,40

Finally, the advantages and disadvantages of hydronic heating systems (radiant panels, radiators) are systematized and synthesized, and in addition, the performance of GCHP, with

double U-tube borehole, connected to different heating/cooling systems (radiant floor, radiant wall and ceiling panels, radiators) of the experimental office, described in detail in the thesis, under the conditions of ensuring adequate thermal comfort. The results show that radiant heating panels work better than heating with radiators. A COP_{syst} = 4.92 was obtained with 6.3%, 7.0% and 7.4% higher with radiant floor heating compared to radiant wall, radiant ceiling and radiator heating respectively (Table 5.11) and a COP_{syst} = 6.11, 5.9% and 39.8% higher for the radiant ceiling cooling system compared to radiant wall cooling and radiant floor cooling, respectively (Table 5.14).

The floor-ceiling combined radiant heating system has the best performance in terms of the lowest electricity consumption and CO_2 emission (COP_{syst} = 5.45; M_{CO_2} =2.15 kg), being closely followed by the radiant floor system. Energy consumption is 43% lower than radiant floor and 66% lower than radiators. The radiant ceiling heating system has the worst performance in terms of the listed parameters (COP_{syst} = 4.60; M_{CO_2} =3.55 kg).

Table 5.11 Performances of experimental heating systems

Heating system	t_e (°C)	t_i (°C)	t_f (°C)	t_t (°C)	E_t (kWh)	E_{el} (kWh)	COP_{syst} (–)	M_{CO_2} (kg)	On/ Off
Radiators	4,96	22,60	15,01	34,61	54,75	11,95	4,58	3,57	168
Radiant floor	4,72	22,31	16,66	32,75	50,62	10,29	4,92	3,08	68
Radiant wall	4,23	22,30	16,38	32,35	54,26	11,72	4,63	3,50	76
Radiant ceiling	5,16	22,35	16,33	32,65	54,60	11,87	4,60	3,55	84
Floor-ceiling	5,28	22,06	17,23	26,98	39,17	7,19	5,45	2,15	62

Table 5.14 Performances of experimental cooling systems

Cooling system	t_e (°C)	t_i (°C)	t_f (°C)	t_t (°C)	E_t (kWh)	E_{el} (kWh)	COP_{syst} (–)	EER_{syst} (Btu/Wh)	M_{CO_2} (kg)
Radiant floor	28,46	26,86	20,47	20,96	42,48	9,72	4,37	14,91	2,91
Radiant wall	28,54	26,29	20,38	20,83	55,05	9,54	5,77	19,69	2,85
Radiant ceiling	28,01	26,07	20,42	20,85	52,52	8,59	6,11	20,85	2,57

After evaluating the interior thermal comfort, using Thermal Comfort software, it is found that the radiant heating systems through the floor and combined floor-ceiling lead to increased thermal comfort compared to the heating systems with radiators, radiant ceiling and radiant wall (lower PMV values by 71–124%, 19.5–31% and, respectively, 0–8.6%), and the radiant wall cooling system leads to increased thermal comfort compared to the radiant floor and ceiling cooling systems radiant (lower PMV values by 31–41% and, respectively 10.4–14.2%).

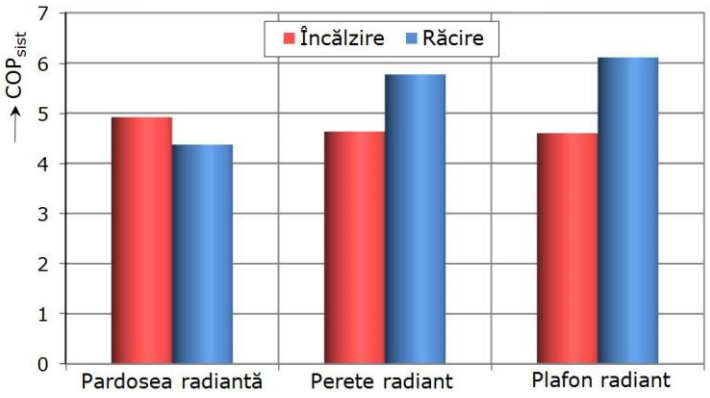

Fig. 5.49 Comparison of the performance coefficient of different radiant heating and cooling systems

From the comparison of the three simple radiant heating/cooling systems analyzed (floor, wall, ceiling) (Fig. 5.49) it follows that the system with the radiant floor in the heating mode, and the system with the radiant ceiling panels in the cooling mode have superior performances, also leading to increased thermal comfort, under the same operating conditions.

6. NUMERICAL SIMULATIONS AND MODELINGS

Chapter 6 is intended to numerical simulations and modeling using the specialized programs briefly described in its first part. Three numerical simulation models were developed in TRNSYS [31], experimentally validated, to determine the useful thermal energy for heating/ cooling and DHW production and to determine the energy efficiency of various heating/ cooling systems connected to a GCHP for maximizing their efficiency and providing users with thermal comfort throughout the year.

To *simulate the thermal energy useful* to cover the heat/cold needs of the experimental office, the operational connections between the building and the internal and external factors were established. Fig. 6.1 illustrates the operational scheme constructed in TRNSYS.

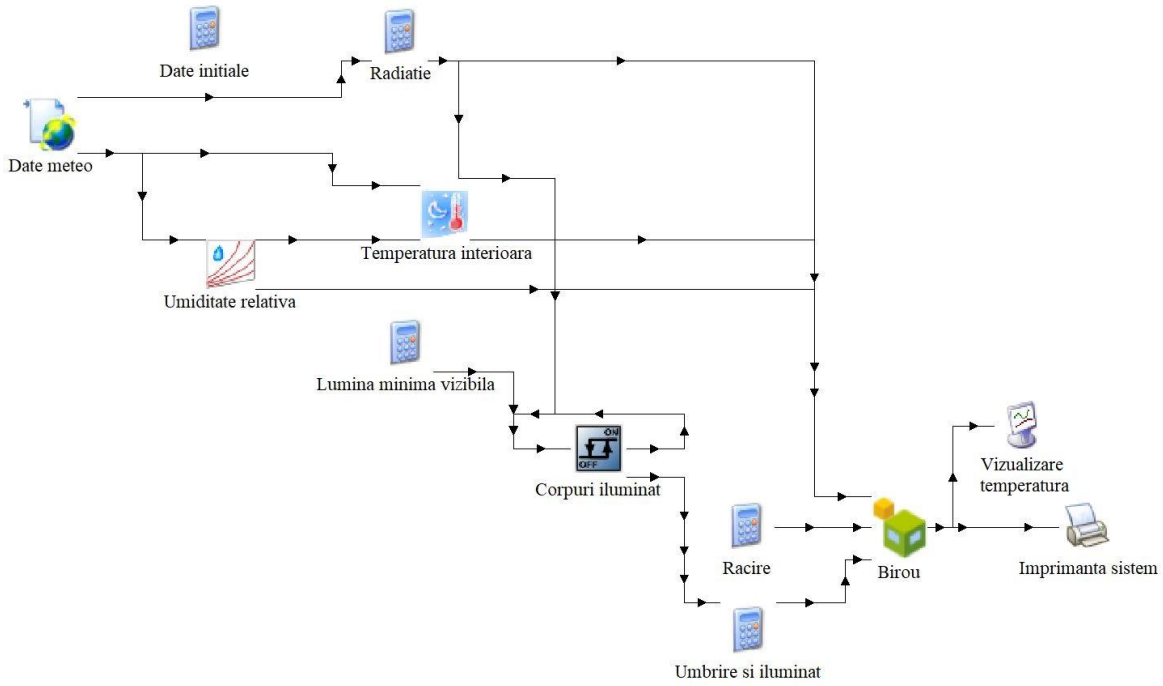

Fig. 6.1 Scheme of the simulation model in TRNSYS of the thermal energy useful in heating and cooling

Performing simulations for a period of one year (8760 h) the values of the thermal energy used for heating and cooling were obtained and presented in Table 6.1 alongside the measured values. Statistical index values: root mean square error (RMSE), coefficient of variation (c_v) and coefficient of multiple determinations (R^2) are included in Table 6.2 for the GCHP system operating in different modes.

It is found that there is a maximum absolute relative error between the TRNSYS simulated values and the measured values of approximately 2.03% during heating and approximately 1.38% during cooling, which is very acceptable. RMSE and c_v values in heating mode are 1.576 and 0.0121, respectively, and in cooling mode are 3.376 and 0.0171, respectively. The R^2 values in the two operating modes are approximately 0.9999 and are considered very satisfactory. Thus, the simulation model was validated by the experimental data.

Table 6.1 Useful thermal energy for heating and cooling

Month	Heating energy (kWh)		Relative error e_r (%)	Cooling energy (kWh)		Relative error e_r (%)
	Simulated	Measured		Simulated	Measured	
January	280.40	275.63	1.70	0.00	0.00	0.00
February	208.71	210.34	0.78	0.00	0.00	0.00
March	88.36	89.36	1.13	0.00	0.00	0.00
April	22.92	23.51	2.57	0.00	0.00	0.00
May	0.00	0.00	0.00	101.23	102.31	1.07
June	0.00	0.00	0.00	154.86	155.24	0.25
July	0.00	0.00	0.00	310.24	305.96	1.38
August	0.00	0.00	0.00	284.61	281.46	1.11
September	0.00	0.00	0.00	137.32	135.74	1.15
October	50.20	49.73	0.94	0.00	0.00	0.00
November	191.58	194.07	1.30	0.00	0.00	0.00
December	228.78	224.14	2.03	0.00	0.00	0.00

Table 6.2 Statistical indices of the useful thermal energy simulation model

Operation mode	RMSE	c_v	R^2
Heating	2.72187	0.01409	0.99990075
Cooling	3.08003	0.02382	0.99977802
DHW	8.50000	0.00464	0.99997906

It is found that there is a maximum absolute relative error between the TRNSYS simulated values and the measured values of approximately 2.03% during heating and approximately 1.38% during cooling, which is very acceptable. RMSE and c_v values in heating mode are 1.576 and 0.0121, respectively, and in cooling mode are 3.376 and 0.0171, respectively. The R^2 values in the two operating modes are approximately 0.9999 and are considered very satisfactory. Thus, the simulation model was validated by the experimental data.

To *simulate the production of DHW*, the operational scheme built in TRNSYS in Fig. 6.2 was used. Simulations of the thermal energy useful for providing the thermal power of the DHW were carried out for three hot water temperatures: 45, 50 and 55 °C. The results of the simulation program are presented alongside the experimental data in Table 6.3, and the RMSE, c_v and R^2 statistical indices are included in Table 6.2.

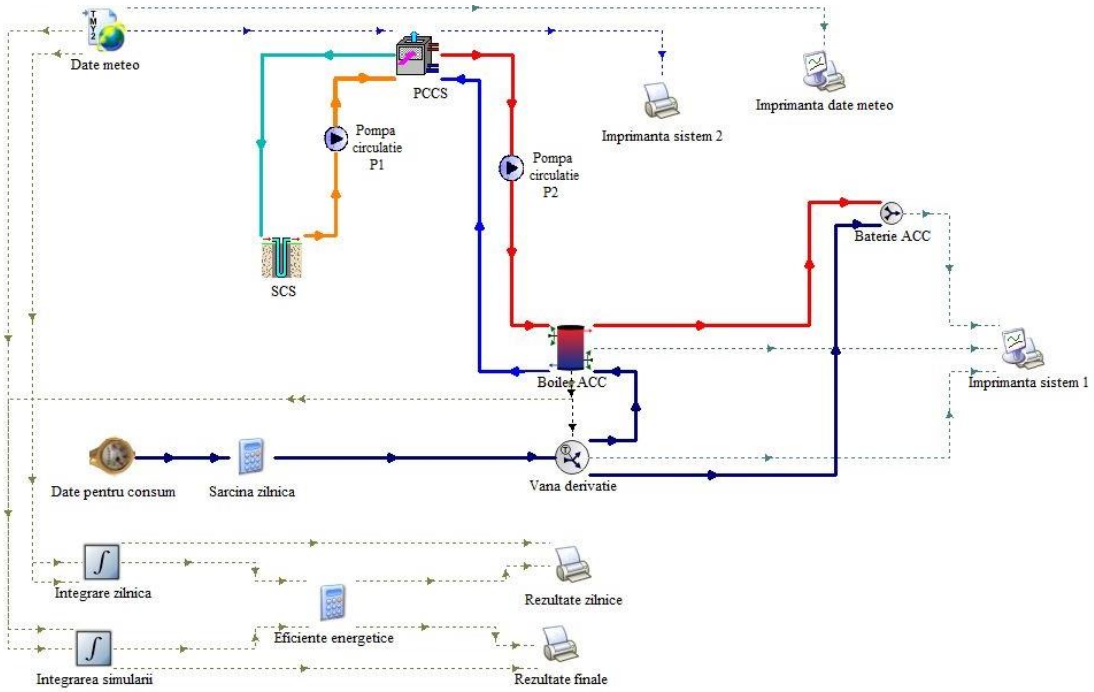

Fig. 6.2 Scheme of the simulation model in TRNSYS of DHW production

Table 6.3 Thermal energy E_t used for DHW production

Temperature $t_{dhw\text{-}set}$ (°C)	E_t (kWh/an)		Relative error e_r (%)	COP_{syst}		Relative error e_r (%)
	Simulated	Measured		Simulated	Measured	
45	1992	1995	0.15	2.14	2.09	2.39
50	2346	2362	0.68	2.06	1.97	6.09
55	2614	2635	0.80	1.87	1.73	8.09

A comparative analysis of these results indicates that the thermal energy values for DHW production simulated with TRNSYS were only 0.15–0.80% lower than the measured values in all three cases. Also, the simulated COP_{syst} values are in the range of 1.87–2.14, close to the measured values, the relative error varying between 2.39% and 8.09%. The R^2 and c_v values of approximately 0.9999 and 0.0058 respectively (Table 6.2) are very satisfactory and thus the simulation model is experimentally validated.

The COP simulation of the heating/cooling systems connected to the PCCS was performed using the operational scheme built in TRNSYS in Fig. 6.3.

Numerical simulation of the COP of a heating system with radiators, simple radiant panels (floor, wall, ceiling) or combined (floor–ceiling) connected to the GCHP, was carried out for a period of one month, and the results obtained in TRNSYS are presented alongside the experimental measurements in Table 6.4. Also, the numerical simulation of the COP_{syst} of each radiant cooling system (floor, wall, ceiling) connected to the GCHP was performed for a period of one month, and the results are summarized alongside the experimental tests in Table 6.5.

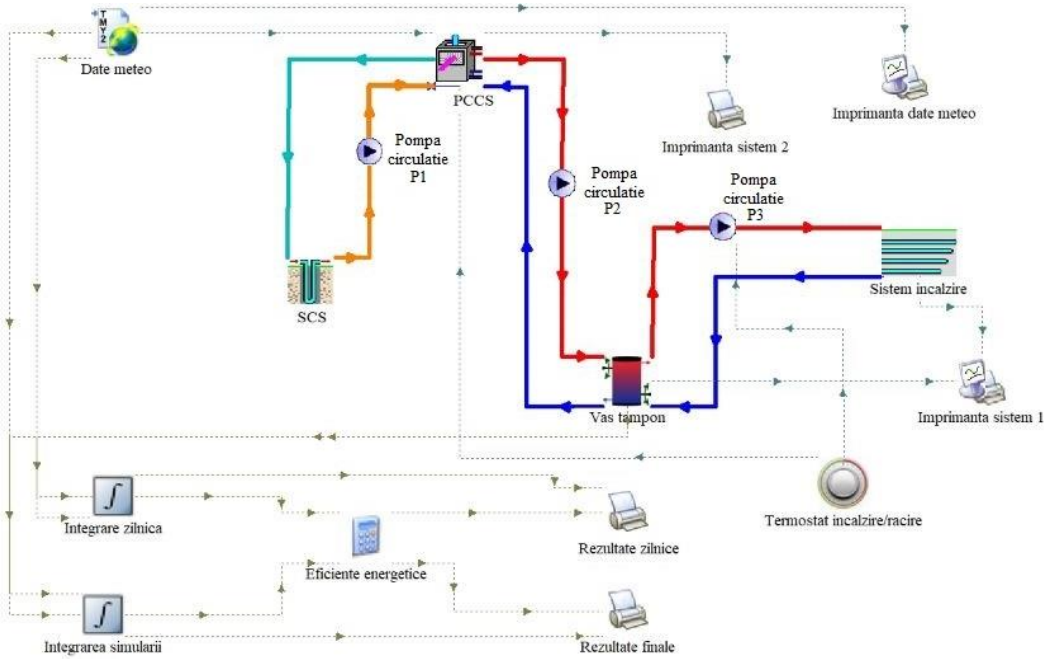

Fig. 6.3 Scheme of the TRNSYS simulation model for the COP of various heating/cooling systems connected to the GCHP

Table 6.4 COP_{syst} values for various heating systems connected to GCHP

Heating system	COP_{syst}		Relative error e_r (%)
	Simulated	Measured	
Radiators	4.72	4.58	3.06
Radiant floor	5.08	4.92	3.25
Radiant wall	4.92	4.63	6.26
Radiant ceiling	486	4.60	5.65
Floor–ceiling	5.68	5.45	4.22

Table 6.5 COP_{syst} values for various cooling systems connected to GCHP

Cooling system	COP_{syst}		Relative error
	Simulated	Measured	e_r (%)
Radiant floor	4.51	4.37	3.20
Radiant wall	5.89	5.77	2.08
Radiant ceiling	6.16	6,11	0.82

The comparative analysis of the results obtained in Table 6.4 shows that the simulated COP_{syst} values are lower by only 3.06% than the measured ones, for the heating system with radiators and only by 3.25%, 6.26%, 5.65% and 4.22% than the measured values, for radiant heating systems through the floor, wall, ceiling and, respectively, combined floor-ceiling. At the same time, the results obtained in Table 6.5 show that the simulated COP_{syst} values are only 3.2% lower than the measured ones, for the radiant floor cooling system and only 2.08% and 0.82% for the radiant wall and ceiling cooling systems, respectively. Thus, the numerical simulation model can be considered experimentally validated.

In addition, a comparative theoretical study with the numerical simulation program Polysun [32] and some experimental investigations on *the performances of a hybrid GCHP-PV/T system with continuous regeneration* by PV/T and a *conventional GCHP system*, integrated in the system of heating and DHW production for both the experimental office and a single-family building was performed.

In the hybrid GCHP-PV/T system (Fig. 6.4) the PV/T panels are used as an additional heat source with GHE. Seasonal performance factors SPF_{HP}, SPF_{syst} and $SPF_{HP\text{-}PV}$ are used to analyze the performance of different GCHP systems through simulation and monitoring.

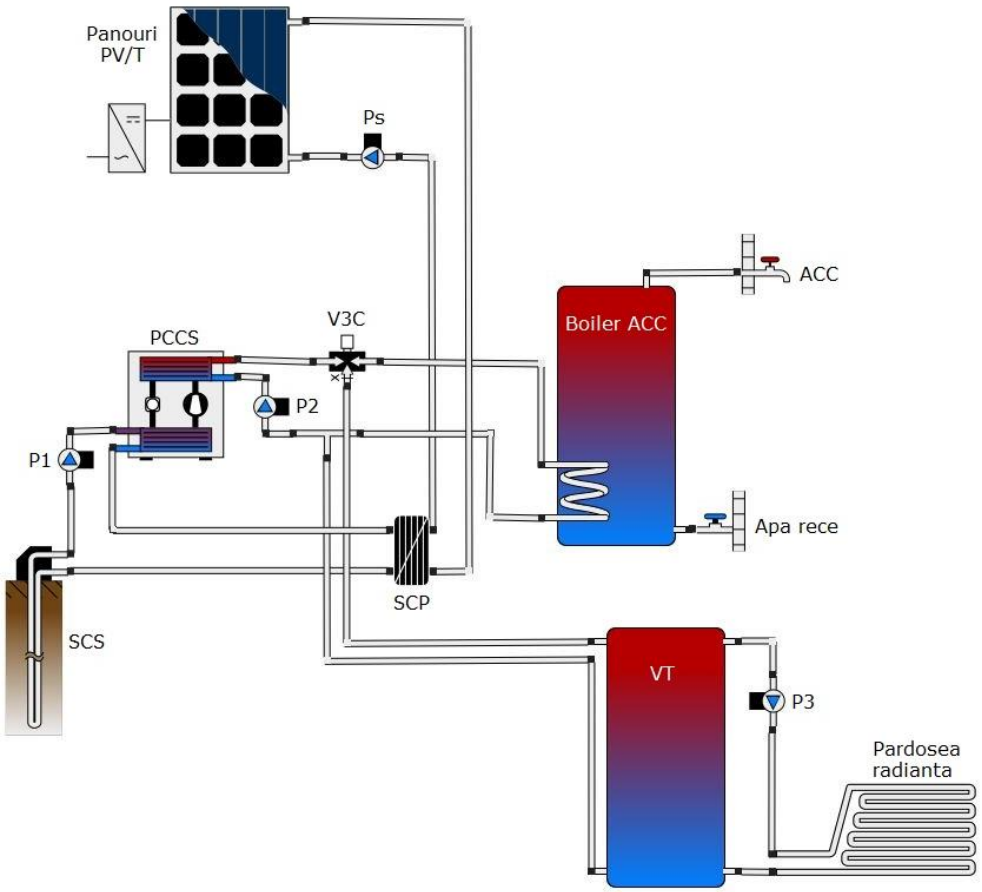

Fig. 6.4 Configuration of the hybrid GCHP-PV/T system for simulation with Polysun program

• *Simulation for the experimental office*. The Polysun program was used to simulate, during March 2021, the thermal energy useful to satisfy the heating and DHW demands for the experimental office and the electricity generated by the PV/T panels, which compensates the electricity used by the HP. Table 6.6 summarizes the main results simulated with the Polysun program alongside the values obtained through experimental measurements.

Table 6.6 GCHP performances interconnected with PV/T panels obtained by simulation and monitoring in heating–ACC mode

Value	E_t (kWh)	$E_{el,pv}$ (kWh)	E_{HP} (kWh)	SPF_{HP} (–)	Reduction of CO_2 emissions (kg)
Simulated	209	54	49	4.26	14.65
Measured	214	57	50	4.28	14.95
Relative error, e_r (%)	2.4	5.6	2.0	0.5	2.0

The results show that the simulated values such as useful thermal energy (E_t), electrical energy produced by PV/T panels ($E_{el,pv}$), electrical energy consumed by HP (E_{HP}), HP seasonal performance factor (SPF_{HP}) and emission reduction of CO_2 are only 0.5–5.6% lower than the measured ones, so that the numerical simulation model is considered experimentally validated.

• *Simulation for a single-family building*. The Polysun program was further used to simulate for a full year the performance of the continuously regenerative hybrid system through an array of 20 PV/T panels, used to supply heat and DHW to a low-energy single-family building, both for double and single U-tube borehole configuration. The array of 20 PV/T panels installed on the roof of the building has an area of 31.8 m^2 and a total nominal power of 4.5 kW. Table 6.7 summarizes the main results simulated with the Polysun program.

Another numerical simulation was performed for the conventional GCHP system (without PV/T regeneration), the main numerical results obtained being included in Table 6.8.

Table 6.7 Performance simulation results of the GCHP-PV/T hybrid system in heating–DHW mode during one year

GHE configuration	E_t (kWh)	$E_{el,pv}$ (kWh)	$E_{PC\text{-}HP}$ (kWh)	E_{HP} (kWh)	E_{el} (kWh)	SPF_{HP} (–)	SPF_{syst} (–)	SF_{PV} (–)	PR_{PV} (–)	SCR (–)	$SPF_{HP\text{-}PV}$ (–)	CO_2 reduction (kg)
(1) Double U-tube	9725	5279	2250	2250	5226	4,32	1,86	1,00	0,79	0,43	5,79	1563
(2) Single U-tube	9725	5279	2131	2131	5203	4,56	1,87	1,00	0,79	0,40	6,00	1556

Table 6.8 Performance simulation results of the conventional GCHP system in heating–DHW mode during one year

GHE configuration	E_t (kWh)	E_{HP} (kWh)	E_p (kWh)	E_{aux} (kWh)	E_{el} (kWh)	SPF_{HP} (–)	SPF_{syst} (–)	CO_2 reduction (kg)
Single U-tube	9834	2090	1756	1680	5526	4,70	1,78	1652

From the analysis of the numerical simulation results with the Polysun program, it was found that the hybrid GCHP-PV/T system achieves electricity savings and CO_2 emission reduction of 6.2% compared to the conventional GCHP system, and the SPF of the system (SPF_{syst}) increases by 5%, from 1.78 to 1.87 although the SPF of HP (SPF_{HP}) drops from 4.70 to 4.56. In addition, the $SPF_{HP\text{-}PV}$ indicator in the single U-tube configuration is 3.6% higher than the double U-tube configuration, and combined HP with PV/T panels (31.8 m^2) leads to CO_2 emission reductions approximately equal (difference below 0.5%) in the two configurations.

The heat pump in combination with the PV/T panels (31.8 m^2) can fully offset the electricity consumption when operating the heating and DHW system of a single-family building throughout the year. Also, the long-term cooling effects of GHE can be eliminated by solar

thermal regeneration with PV/T panels, leading to shorter GHEs and an increase in soil temperature and thus ensuring sustainable system operation.

7. ECONOMIC-ENERGY AND ENVIRONMENTAL IMPACT STUDY OF HEATING AND COOLING OF AN EXISTING BUILDING WITH DIFFERENT ENERGY SOURCES

In *chapter 7*, a comparative economic, energetic and environmental study is carried out for heating and cooling an existing multifunctional building with various primary energy sources such as closed-loop GCHP, air-water HP (AWHP), thermal plant (TP) with natural gas and TP with pellets, justifying the opportunity of the closed-loop GCHP heating and cooling solution with vertical collectors.

It is considered an existing building (without insulation of the external walls) with P+2E height regime and having a total area of 1560 m^2, located in Timisoara, intended for students' study, with classrooms, offices, computer science, physics and chemistry laboratories on each level, as well as sanitary groups.

The heat demand for the building was determined in accordance with SR 1907-1/2014, and the cold demand in accordance with SR 6648-1/2014, resulting in a heating thermal power of 108 kW and a cooling thermal power of 132 kW, respectively. The thermal power required for DHW production, calculated according to the Mc 001/2-2006 methodology, is 21 kW.

The thermal energy consumed monthly to satisfy the heating and cooling power of the building was determined according to the NP 048-2000 standard, and respectively the Mc 001/4-2006 methodology, and were graphically represented in Fig. 7.1.

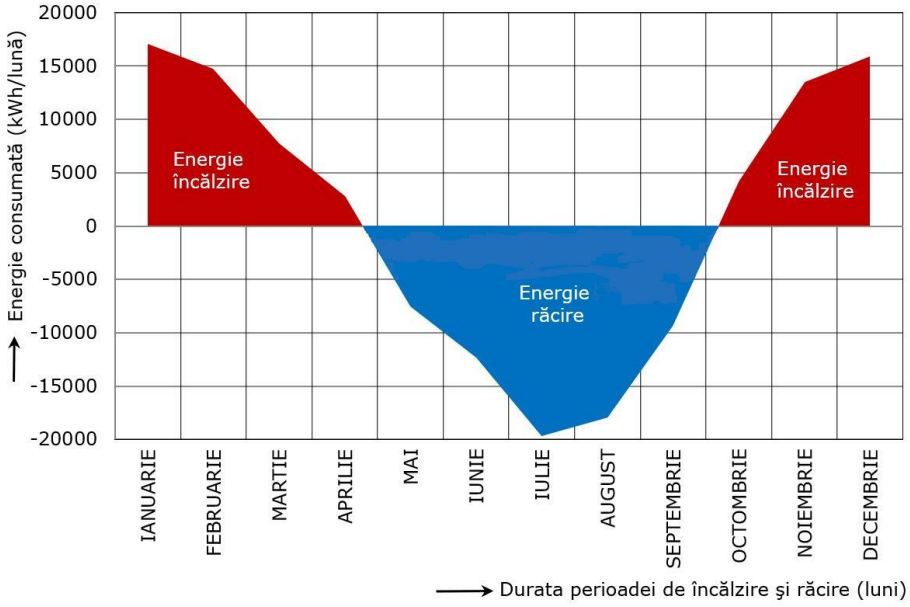

Fig. 7.1 Monthly thermal energy consumption for heating and cooling the building

• *Description of the proposed solution*. A new, fully equipped and automated thermal plant (TP) is being built for heating and cooling the building. TP is equipped with a system of two HPs with a thermal power of 66 kW each, coupled to the ground in a closed loop (Fig. 7.2). The heat pumps have a scroll compressor and work with ecological freon R-410A covering the entire heat and cold demands of the building and the heat demand for the production of DHW. Each HP exchanges heat with the ground through 9 boreholes, each 100 m long and 150 mm in diameter, which each include a 32 mm diameter PEHD double U-tube. The distance between boreholes is 5 m.

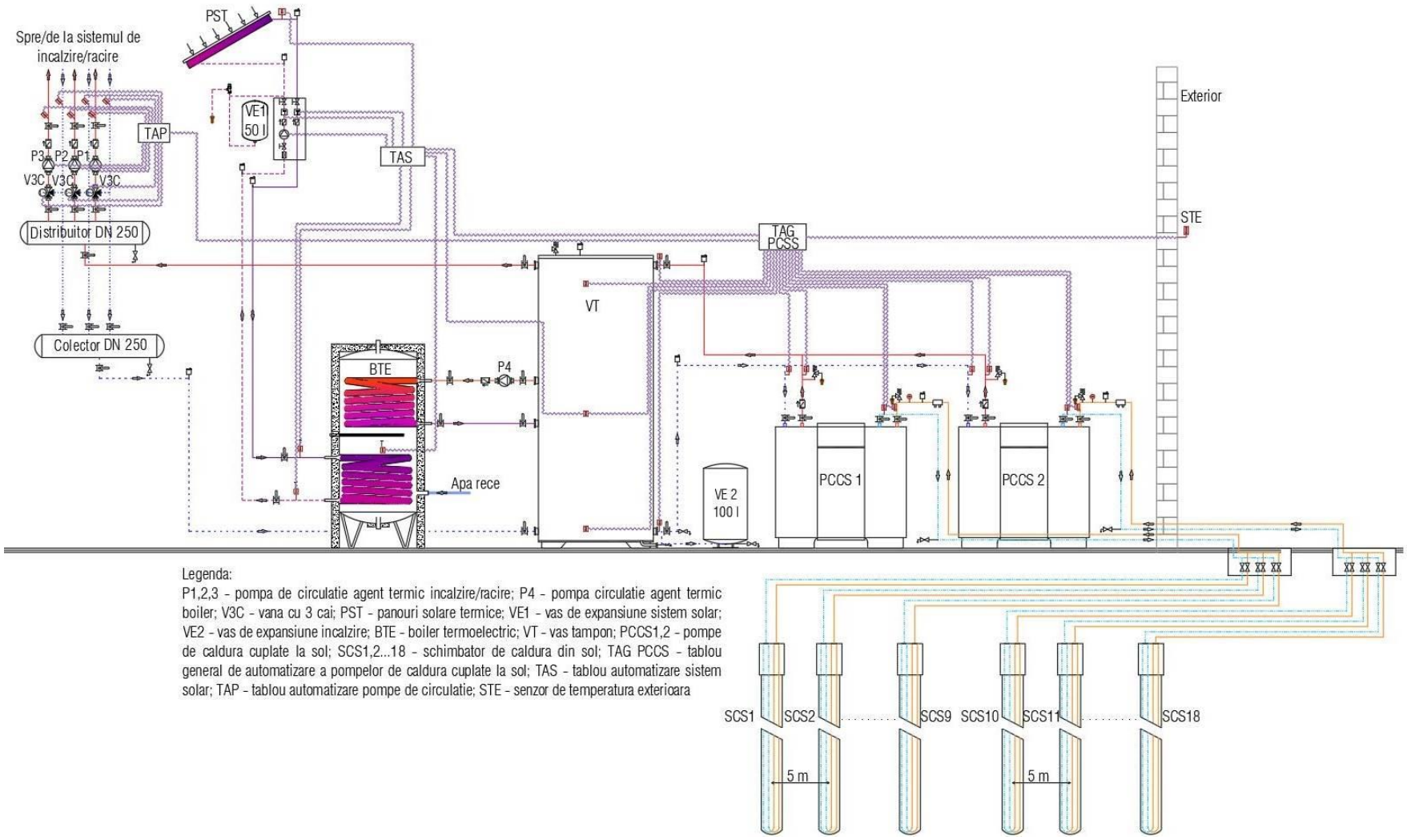

Legenda:
P1,2,3 - pompa de circulatie agent termic incalzire/racire; P4 - pompa circulatie agent termic boiler; V3C - vana cu 3 cai; PST - panouri solare termice; VE1 - vas de expansiune sistem solar; VE2 - vas de expansiune incalzire; BTE - boiler termoelectric; VT - vas tampon; PCCS1,2 - pompe de caldura cuplate la sol; SCS1,2...18 - schimbator de caldura din sol; TAG PCCS - tablou general de automatizare a pompelor de caldura cuplate la sol; TAS - tablou automatizare sistem solar; TAP - tablou automatizare pompe de circulatie; STE - senzor de temperatura exterioara

Fig. 7.2 Scheme of the GCHP system through vertical heat exchangers for heating/cooling the multifunctional building

The heating and cooling of the classrooms, offices and laboratories is done with two-pipe ceiling cassette fan coil units, and in the sanitary groups for heating, compact steel radiators are used. The supply/return temperatures of the heat carrier provided by HPs for heating with fan coils and radiators are 50/40 °C. The thermal cooling agent required for ceiling-mounted fan coils is provided by HPs at supply/return temperatures of 8/13 °C.

The distribution of the heating/cooling facility is done through the false ceiling of each building level with steel pipes insulated with porous rubber, having a thickness of 13 mm.

To reduce energy costs and pollutant emissions, when preparing DHW during the summer in each solution, a solar system composed of 6 thermal panels, pumping group, expansion tanks and the automation module is connected to the boiler.

• *Cost analysis*. Tables 7.2 and 7.3 present the estimated values of the initial investment costs and operating costs during the life of the system for various primary energy sources (GCHP, AWHP, TP with gas, TP with pellets). Gas and pellet TPs each use a chiller for cooling. Equipment costs are predominant in each solution. The costs of the GCHP and AWHP systems are based on the prices provided by the renowned manufacturer Stiebel Eltron, and the average borehole execution costs are considered to be 20 €/m for clay shales.

Table 7.4 presents an economic analysis based on the present cost method for the operation period, considered τ = 20 years. Eq. (2.30) was used to find out the value of the present cost PC, in which TAC=I_0+C_{ex} and the inflation rate β_0 = 10% were entered, which leads to the update rate u_r =8.51.

Table 7.2 Initial investment costs I_0, in €, for various building heating/cooling solutions

Solution components	Heat pump (HP)		Thermal plant (TP)	
	GCHP	AWHP	Gas	Pellets
HP/TP	62,586	66,419	8060	6860
Boreholes	36,000	–	–	–
GHEs	5310	–	–	–
Chiller	–	–	31,400	31,400
Solar system	3600	3600	3600	3600
Gas connection	–	–	2830	–
Chimney	–	–	1410	1410
Buffer tanks	2280	2280	2280	2280
Circulation pumps	5920	5920	5920	5920
Total investiție	115,696	77,949	55,500	51,470

Table 7.3 Operation and maintenance costs C_{ex} for various building heating/cooling solutions

Solution characteristics	GCHP		AWHP		TP		Chiller
	Heating	Cooling	Heating	Cooling	Gas	Pellets	Cooling
Installed thermal power (kW)	132	144	142	138	150	150	135
Efficacy /COP (-)	4,56	3,50	3,20	2.94	0,90	0,80	2,97
Annual operation (h/an)	1700	350	1700	350	1700	1700	350
Electricity price (€/kWh)/ Fuel price (€/m^3)	0,18	0,18	0,18	0,18	0,65	0,39	0,18
Fuel calorific power (kWh/m^3), (kWh/kg)	–	–	–	–	10,42	5,00	–
Annual energy consumption (m^3/an), (kg/an)	–	–	–	–	27.191	63.750	–
(kWh/an)	49.210	14.400	75.438	16.429	283.330	318.750	15.909
Annual operation cost, C_{ex} (€/an)	8858	2592	13.579	2957	17.674	24.862	2864

Table 7.4 Cost analysis

Cost (€)	Heat pump (HP)		Thermal plant (TP)	
	GCHP	AWHP	Gas	Pellets
Total investment cost, *I*	115,696	77,949	55,500	51,470
Annual operation cost, C_{ex}	11,450	16,536	20,538	27,726
Operating cost after 20 years	97,485	140,787	174,860	236,059
Present cost, PC	1,082,521	804,445	647,396	674,275

The numerical results show that the lowest present cost value is obtained in the case of TP with gas, followed by the TP with pellets. The energy cost after 20 years of the GCHP system operation, of €97,485, is much lower than in the solutions using TP with pellets (58.7%), TP with gas (44.2%) and AWHP (30.8%). Additionally, from the performed calculations, it is found that compared to any of the three analyzed solutions, the closed-loop GCHP system has a payback time RT of the additional investment lower than the normed recovery time RT_n, of 8 years.

- *Annual energy consumption*. For heating, the annual energy consumed by the closed-loop GCHP system is 35% lower than the AWHP system, 83% lower than gas TP and 85% lower than pellet TP. In addition, the cooling electricity saving recorded when using the GCHP system is 12.3% compared to the AWHP system and 9.5% compared to the classic TP gas or pellet systems.

- *The CO_2 emissions* of the GCHP system are compared with those of the AWHP system and with those of some systems that use a gas TP or a pellet TP for heating and a conventional chiller for cooling. The CO_2 emissions of the four analyzed systems were calculated based on the specific emission factor and summarized in Table 7.5.

Table 7.5 CO_2 emissions of heating/cooling systems analyzed

System	Electrical energy (kWh)	Natural gas (kWh)	Pellets (kWh)	M_{CO_2} (kg)
GCHP	63,610	–	–	19,019.4
AWHP	91,867	–	–	27,468.2
Gas TP	15,909	283,330	–	62,839.5
Pellet TP	15,909	–	318,750	129,069.3

From the analysis of the numerical results, it is found that the GCHP system uses the least energy in operation compared to the other three heating/cooling systems, contributing to the conservation of natural resources. That is why the CO_2 emission of this system (M_{CO_2} = 19,019.4 kg) is reduced by 30.8% compared to the AWHP system and by 67.7% and 85.3%, respectively, compared to the classic TP systems with gas or pellets.

8. FINAL CONCLUSIONS, CONTRIBUTIONS AND NEW DIRECTIONS FOR EXPLORATION

Chapter 8 contains the main general conclusions of the bibliographic, theoretical and experimental research, demonstrating higher performance of the GCHP system in the case of using double U-tube borehole compared to the single U-tube borehole case and showing possible improvements in the energy performance of some heating/cooling systems connected to closed-loop GCHP with vertical GHE and CO_2 emission reductions, as well as the author's personal contributions and potential new research directions and promotion of the proposed concepts.

8.1 Final conclusions of the research. The theoretical studies, numerical analyzes and experimental research carried out by the author in this doctoral thesis during the last seven years of scientific activity in the Department of Civil and Building Services Engineering had the main purpose of ensuring the energy efficiency of thermal systems and comfort in civil buildings along with reducing CO_2 emissions using GCHP. After conducting *bibliographic research*, the following general conclusions can be formulated:

1) In the current energy conditions, as the degree of provision with conventional energy resources is reduced, the interest in RES continues to grow, of which HP represents a viable alternative to the preparation of heat carrier for heating/cooling and of DHW, especially in the case of modern constructions with improved thermal insulation, also having a significant role in reducing CO_2 emissions.

2) To determine the technical and economic efficiency of heat production in a HP installation, a series of economic and energy indicators must be used on the basis of which the heat production solution with HPs can be compared with other solutions.

3) The COP of a HP is the higher the smaller the difference between the heat medium temperature for the heating/cooling system and the cold source temperature, and the use of HP in heating/cooling is justified when the synthetic rentability indicator $\eta_s > 1$ and energy efficiency $COP_{HP} > 2.875$.

4) The use of soil as a heat source for HPs has the advantage that the source is almost completely independent of heat demands and does not have a minimum thermal power in the cold season, unlike other natural sources.

5) For new buildings, the monovalent operating mode of HP is used, which can be interrupted without changing the comfort temperature due to the storage capacity of the radiant heating systems. For old buildings, the bivalent operating mode of the HP is used as there is an auxiliary heat source, which covers the peak loads, when the temperatures on the circuit exceed 55 °C.

6) In hot climate regions, where cooling is dominant, combining a GCHP system for cooling with a GCHP system for DHW production becomes very advantageous in terms of energy performance, for buildings with high thermal energy consumption and high hot water demand, especially in summer, such as commercial buildings and hospital and hotel buildings. In addition, hybrid GCHP systems with DHW production can be an alternative for residential and commercial buildings.

7) The long-term cooling effects of GHEs can be eliminated by solar thermal regeneration with PV/T panels, leading to shorter GHEs and an increase in soil temperature and thus ensuring sustainable system operation.

After *conducting theoretical and experimental research*, the following were concluded:

1) Finding the refrigerants that lead to high HP performance can be done using the *Z*-inefficiency proposed by the author, which includes sensible and latent heat and the operating temperatures of the refrigerant in the installation. For this purpose, the COP-*Z* correlations for heating and cooling, corresponding to several refrigerants, have been developed.

2) By serialized mechanical vapor compression HP, the electricity consumption can be reduced by approx. 33%.

3) In the case of buildings with a dominant heating load, the use of a solar photovoltaic/thermal (PV/T) panel can greatly reduce the depth of the borehole, thus also the cost of GHE installation. The newly introduced seasonal performance factor $SPF_{HP\text{-}PV}$ for the hybrid HP-PV/T system combines the performance quality of the HP, the PV generator and the integration of the two subsystems.

4) Experimental research has demonstrated higher performance of the GCHP system

when using the double U-tube borehole compared to the single U-tube configuration (COP_{syst} increases by 3–8% and CO_2 emission decreases by 5–10%).

5) The GCHP system operating in heating mode has a COPsyst > 5, and in cooling mode a $COP_{syst} \cong 4$, and the GCHP system operating in heating/cooling and DHW mode has a $3 < COP_{syst} < 4$, for both cases.

6) In the single and double U-tube configurations, the COP_{HP} values for the heating and DHW providing tests were 3.56 and 3.66, respectively, and for the heating tests, they were 5.82 and 6.08, respectively.

7) When using the double U-tube, electricity savings and CO_2 emission reductions of 6.5% for office heating, 3.2% for office cooling and 5% for office cooling simultaneously with the DHW production.

8) If the GCHP is used to produce only DHW for a family at different temperatures between 45 and 55 °C, then the COP_{HP} would decrease to approximately 1.8–2 and the CO_2 emission value would vary between 6.02 and 9.47 kg in the double U-tube configuration and between 5.85 and 8.95 kg in the single U-tube configuration.

9) The experimental results show an increase in the average temperature of the working fluid by 2.4% and an improvement in the performance of the office heating system connected to the GCHP with regeneration by injecting heat into the soil in the summer season (in the GHE configuration with single U-tube 3.5% higher COP_{syst} and 1.2% lower CO_2 emission, and in the double U-tube GHE configuration 6.6% higher COP_{syst} and 3.8 lower CO_2 emission).

10) After the injection of heat into the soil, the highest increase in COP_{syst} is also obtained for the double U-tube borehole configuration compared to the single U-tube, of 7.7%, as well as the highest CO_2 emission reduction of 6,9% The thermal imbalance ratio, TIR = 0.054 shows that the thermal balance of the soil is good enough and the performance can be kept approximately constant.

11) The experimental study showed that radiant heating panels work better than heating with radiators. The four simple heating systems have relatively small differences (maximum 7.4%) in the value of their energy performance coefficient (COP_{syst} equal to 4.92, 4.63, 4.60 and 4.58 for radiant floor, radiant wall, radiant ceiling and radiators, respectively), but radiator heating requires more than twice as many on/off as radiant floor heating, leading to higher HP wear. In addition, the energy consumption and CO_2 emission of the heating system with radiators are 16%, 2% and 0.7% higher than the heating system with radiant floor, radiant wall and radiant ceiling, respectively, under the same conditions of operation.

12) The combined floor-ceiling radiant heating system has the best performance in terms of the lowest electricity consumption and CO_2 emission (COP_{syst}= 5.45; M_{CO_2} =2.15 kg), being closely followed by the system with radiant floor. Energy consumption is 43% lower than radiant floor and 66% lower than radiators. The radiant ceiling heating system has the worst performance in terms of the listed parameters (COP_{syst}=4.60; M_{CO_2} =3.55 kg).

13) Radiant ceiling cooling system has the best COP_{syst} of 6.11, 39.8% higher than radiant floor cooling system, equal to 4.37 and only 5.9% compared to radiant wall cooling, equal to 5.77. Also, the electricity consumption and CO_2 emission values are lower by 13% and 11% for the radiant ceiling cooling system compared to the radiant floor and wall cooling systems, respectively, under the same operating conditions.

14) The floor-ceiling combined radiant heating system achieves the best thermal comfort, the PMV index being approximately 0 for personal parameters i_M = 1.1 met and R_{cl} = 0.29 clo (writing, light clothing) and almost 0 for pair 1 met – 0.90 clo (read sitting, winter clothing), same as in case of radiant floor. These two radiant systems are closely followed by the radiant

wall heating system (PMV higher by 0–8.6%), and heating with radiators leads to the lowest thermal comfort (PMV higher by 71–124%), followed by of radiant ceiling heating (PMV higher by 19.5–31%).

15) The radiant wall cooling system creates a high degree of thermal comfort (PMV values, for pair 1 met–0.9 clo, lower by 31–41% compared to the radiant floor cooling system and by 10.4–14.2% compared to the one with a radiant ceiling), being followed by the radiant ceiling.

16) A comparative analysis of the simulation results in TRNSYS indicates that there is a maximum absolute relative error of approximately 2.03% for the heating period and approximately 1.38% for the cooling period between the simulated and measured thermal energy values and that the thermal energy values for the simulated DHW production were only 0.15–0.80% lower than the measured values for all three hot water temperatures considered: 45, 50 and 55 °C. Also, the simulated COP_{syst} values are higher by only 2.39– 8.09% than the measured ones, for heating systems and by 0.82–3.2%, for radiant cooling systems.

17) The three TRNSYS simulation models created can be used as a tool to evaluate the performance of different hydronic heating and cooling systems connected to a GCHP to maximize their energy efficiency and guarantee user comfort throughout the year.

18) From the analysis of the numerical simulation results with the Polysun program, it was found that the hybrid GCHP-PV/T system achieves an electricity saving and CO_2 emission reduction of 6.2% compared to the conventional GCHP system, and the SPF of the system (SPF_{syst}) increases by 5%, from 1.78 to 1.87 although the SPF of HP (SPF_{HP}) drops from 4.70 to 4.56. In addition, the SPFHP-PV indicator in the single U-tube configuration is 3.6% higher than that in the double U-tube configuration, and HP combined with PV/T panels (31.8 m^2) leads to emission reductions of CO_2 approximately equal (difference below 0.5%) in the two configurations, such that the optimal configuration of the GHE within the hybrid system with regeneration can be considered the simple U-tube.

19) By interconnecting an array of PV/T panels with GCHP integrated into the heating system and producing DHW for a single-family building it is possible to fully offset the electricity consumed during the operation of the system throughout the year.

20) The energy cost after 20 years of operation of the closed-loop GCHP system for heating/cooling an existing non-insulated multifunctional building is 58.7%, 44.2% and 30.8% lower than in solutions using pellet TP, gas TP and AWHP, respectively. Additionally, compared to any of the three analyzed solutions, the GCHP system has a payback time of the additional investment lower than the standard payback time of 8 years.

21) For heating the existing building, the closed-loop GCHP system has an annual energy consumption of 35% less than the AWHP system, 83% less than the gas TP and 85% less than the pellet one. In addition, the cooling electricity saving recorded when using the GCHP system is 12.3% compared to the AWHP system and 9.5% compared to the classic TP gas or pellet systems. The CO_2 emission of the GCHP system (M_{CO_2} = 19,019.4 kg) is reduced by 30.8% compared to that of the AWHP system and by 67.7% and 85.3%, respectively, compared to that of the classic TP systems with gas or pellets.

8.2 Original contributions:

1) Definition of various energy, economic and environmental performance indicators for the implementation of HP with electro-compressor in heating/cooling systems.

2) Performing a study on the recent development of possible substitutes for non-environmental refrigerants and their effectiveness on the COP of HP, as well as proposing a simple and fast method for calculating the COP of HP based on the vaporization and condensation temperatures of the refrigerant and the number Jacob, which includes the specific heat of the

liquid refrigerant and the latent heat of condensation.

3) Realization of an extensive documentary synthesis on geothermal HPs focused on closed-loop GCHP, synthesis of the main numerical and analytical models for simulating vertical GHE inside and outside the borehole, as well as a brief description of some of their design/simulation programs.

4) Carrying out a theoretical study on the hybrid GCHP system combined with photovoltaic-thermal (PV/T) collectors and proposing a new seasonal performance factor (SPF_{HP-PV}), specific to hybrid HP-PV/T systems, which includes the integration of HP subsystems and PV generator and the renewable character of HP-PV/T.

5) Construction of borehole and double U-tube vertical GHE connected to reversible HP with electro-compressor, as well as design and execution of radiant wall and ceiling panel heating/cooling systems for experimental investigations.

6) Conception and realization of the geothermal-solar test facility and experimental research program for GCHPS heating/cooling systems.

7) Performance testing of an experimental vertical GCHP system operating in heating, cooling and DHW production mode, both in the case of using double and single U-tube boreholes.

8) Experimental investigation of GCHP performances with regenerative soil injection in the summer season, using double and single U-tube boreholes, of thermal energy from a boiler, driven by electricity produced by six PV panels.

9) Formulation of a heat transfer simulation model between the vertical GHE and the soil, in both double and single U-tube configurations, that can be solved by the implicit Crank-Nicolson finite difference numerical method, using the MATLAB or FORTRAN programming environment.

10) Experimental evaluation of GCHP performances, with double U-tube borehole, connected to different heating/cooling systems (radiant floor, wall and ceiling radiant panels, radiators) of the experimental office, under the conditions of ensuring adequate thermal comfort.

11) Description of an indoor thermal comfort model based on PMV-PPD indices and their simulation for different pairs of personal parameters i_M and R_{cl} at various points of the heated/cooled space of the experimental office, using commercial Thermal Comfort software.

12) Development of numerical simulation models in TRNSYS for determining the thermal energy useful for heating, cooling and DHW production and evaluating the performance of GCHPs connected to different heating/cooling systems to optimize their energy efficiency.

13) Performing a comparative theoretical study with the numerical simulation program Polysun on the performances of a hybrid GCHP-PV/T system with continuous PV/T regeneration by PV/T and a conventional GCHP system, for the heat and DHW supply of the experimental office and a single-family building.

14) Validation of numerical simulation models in TRNSYS and Polisun programs with the experimental measurements.

15) Carrying out a comparative economic-energy and environmental analysis for the heating and cooling of an existing multifunctional building with various primary energy sources, justifying the opportunity of the heating and cooling solution with a system of two closed-loop GCHP through nine heat exchangers vertical with double U-tube.

The partial results of the theoretical studies and experimental investigations undertaken during the development of the doctoral thesis were valorized by the publication/submission for publication of 10, respectively 2 articles, in specialized journals from the country and abroad with an impact factor, indexed by Clarivate Analytics/Web of Science and in the proceedings of national and international conferences, indexed by BDI. The published papers received a total of 226 independent citations, of which 186 were indexed in Clarivate Analytics/Web of Science and 40 indexed in SCOPUS.

8.3 Potential new research directions. The following research directions with potential for future approach were identified:

1) Conducting experimental investigations to validate the heat transfer simulation model between the vertical GHE and the ground, in double and single U-tube configuration and the comparative analysis between the thermal performance of GHE with two independent circuits for the double and single U-tube in heat injection and heat extraction mode of operation.
2) Performing a study to allow the simulation of HP operation with various refrigerants and the implementation of operating cycles with several compression stages.
3) For a possible improvement of the GCHP system energy efficiency, in-depth research is needed, aimed at the integration of solar PV panels into the system, to produce the electricity needed to drive the circulation pumps in the water pumping process and auxiliary equipment.
4) Carrying out further investigations to examine other low-temperature heating systems and their combinations to be interconnected in geothermal-solar systems.
5) For the analyzed hybrid GCHP-PV/T system, it is important to optimize design schemes and operation strategies from the viewpoint of long-term performance.
6) Since the current hybrid PCCS-PV/T systems mainly use flat PV/T panels, future research of these systems with advanced PV/T types, such as high-temperature PV/T collectors, which can be used for applications with higher temperature requirements.
7) Another future direction of research that is becoming more and more important in the current energy conjuncture is the integration of GCHP in connection with other RES in the 5th generation centralized heating systems.

SELECTIVE BIBLIOGRAPHY

[1] Sarbu I. Advances in building services engineering: Studies, researches and applications. Springer, Cham, Switzerland, 2021.
[2] Sarbu I, Mirza M, Muntean D. Integration of renewable energy sources into low-temperature district heating systems: A review. Energies 2022;15(18):art.6523.
[3] Sarbu I, Dorca A. Review on heat transfer analysis in thermal energy storage using latent heat storage systems and phase change materials. International Journal of Energy Research 2019; 43(1):29-64.
[4] Zamfir Al. Management of renewable energy and regional development: European experiences and steps forward. Theoretical and Empirical Researches in Urban Management 2011;6(3):35-42.
[5] GECR. Kyoto protocol to the United Nations framework conservation on climate change. Global Environmental Change Report, New York, USA, 1997.
[6] EC. Directive 2002/91/EC of the European Parliament and of the council of 16 December 2002 on the energy performance of buildings, Official Journal of the European Communities, 2003.
[7] Sarbu I, Sebarchievici C. General review of ground-source heat pump system for heating and cooling of buildings. Energy and Buildings 2014;70(2):441-454.
[8] Gao B, Zhu X, Yang X, Yuan Y, Yu N, Ni J. Operation performance test and energy efficiency analysis of ground-source heat pump systems. Journal of Building Engineering 2021;41: art. 102446.
[9] Self SJ, Reddy BV, Rosen MA. Geothermal heat pump systems: status review and comparison with other heating options. Applied Energy 2013;101(1):341-348.
[10] Sarbu I, Sebarchievici C. Ground-source heat pumps: Fundamentals, experiments and applications. Elsevier, Oxford, UK, 2016.
[11] Lungu CI. Optimizarea energo-economică a unui sistem de condiționare a aerului utilizând o mașină frigorifică cu absorbție acționată cu gaze naturale. Teză de doctorat, Universitatea Tehnică de Construcții, București, 2004.

[12] Thuesen GJ, Fabrycky WJ. Engineering economy. Prentice-Hall International Editions, 1989.
[13] Sarbu I, Sebarchievici C. Pompe de căldură. Editura Politehnica, Timișoara, 2010.
[14] Philappacopoulus AJ, Berndt ML. Influence of rebounding in ground heat exchangers used with geothermal heat pumps. Geothermic 2001;30(5):527-545.
[15] Simms RB, Haslam SR, Craig JR. Impact of soil heterogeneity of horizontal ground heat exchangers. Geothermics 2014;50:35-43.
[16] Ingersoll LR, Adler FT, Plass HJ, Ingersoll AC. Theory of earth heat exchangers for the heat pump. ASHRAE Transactions 1950;56:167-188.
[17] Carslaw HS, Jaeger JC. Conduction of heat in solids. Claremore Press, Oxford, UK, 1946.
[18] Eskilson P. Thermal analysis of heat extraction boreholes. Doctoral thesis, University of Lund, Lund, Sweden, 1987.
[19] Paul ND. The effect of grout thermal conductivity on vertical geothermal heat ex-changer design and performance. M.Sc. Thesis. South Dakota University, Vermillion, SD, USA, 1996.
[20] Pahud O, Hellstrom G, Mazzarella L. Heat storage in the ground: Duct ground heat storage model for TRNSYS, User Manual. Ecole Polytechnique Federale de Lausanne, Lausanne, Switzerland, 1996.
[21] Sharqawy MH, Mokheimer EM, Badr HM. 2009. Effective pipe-to-borehole thermal resistance for vertical ground heat exchangers. Geothermics 2009;38:271–277.
[22] Kerme ED, Fung AS. Heat transfer analysis of single and double U-tube borehole heat exchanger with two independent circuits, Journal of Energy Storage 2021;43: art. 103141.
[23] Zeng H, Diao N, Fang Z. Heat transfer analysis of boreholes in vertical ground heat exchangers, International Journal of Heat and Mass Transfer 2003;46:4467–4481.
[24] Nellis G, Klien S. Heat transfer, Cambridge University Press, Cambridge, 2009.
[25] Lorenzo C, Narvarte L. Performance indicators of photovoltaic heat pumps. Heliyon 2019;5:art.e02691.
[26] SR 1907/1. Instalații de încălzire. Necesarul de căldură de calcul. Metoda de calcul, Asociația de Standardizare din România, București, 2014.
[27] SR 6648/1. Instalații de ventilare și climatizare. Calculul aporturilor de căldură din exterior şi al sarcinii termice de răcire (sensibilă) de calcul al încăperilor unei clădiri climatizate, Asociația de Standardizare din România, Bucureşti, 2014.
[28] NP 048. Normativ pentru expertizarea termică și energetică a clădirilor existente și a instalațiilor de încălzire și preparare a apei calde de consum aferente acestora, Ministerul Dezvoltării Regionale și Administrației Publice, București, 2000.
[29] Mc 001/4. Metodologie de calcul al performanței energetice a clădirilor și apartamentelor, Ministerul Dezvoltării Regionale și Locuinței, București, 2009.
[30] Mc 001/2. Metodologie de calcul al performanţei energetice a clădirilor (instalaţiile din clădiri), Ministerul Dezvoltării, Lucrărilor Publice și Locuințelor, Bucureşti, 2006.
[31] TRNSYS 17. A transient system simulation program user manual. Solar Energy Laboratory, University of Wisconsin-Madison, Madison, USA, 2012.
[32] Polysun Software. User manual, Vela Solaris AG, Wintterthur, Switzerland, 2020.